ACTIVATED CARBON FROM WASTE PAPER FOR THE REMOVAL OF CONTAMINANTS FROM WASTEWATER

A THESIS SUBMITTED IN FULL FULFILLMENT

OF THE REQUIREMENTS FOR THE DEGREE OF

MASTER OF SCIENCE (CHEMISTRY)

OF

THE UNIVERSITY OF NAMIBIA

BY

VIOLA-DE-AMOR CHANTALL PATRICIA WILLEMSE

201408962

OCTOBER 2025

MAIN SUPERVISOR: PROF. ATEEQ RAHMAN (University of Namibia)

CO-SUPERVISOR: DR. KATHITHILENI M. KALILI (University of Namibia)

Abstract

Water pollution is a critical global issue caused by toxic industrial pollutants that threaten both human health and the environment. These contaminants include organic compounds (such as dyes, pesticides, surfactants, and pharmaceuticals) and inorganic substances like sulphates, nitrates, chlorides, and phosphates. Among the treatment methods available, activated carbon (AC) stands out for its high adsorption capacity and cost-effectiveness.

This study aimed to produce activated carbon from waste copy paper using physical and chemical activation methods, with 5% phosphoric acid used for chemical activation. Waste paper was first de-inked using a flotation solution of 1% sodium hydroxide, 1% sodium silicate, and oleic acid, followed by pyrolysis at 600 °C for 2 hours. The resulting ACs were characterised using Fourier-transform infrared spectroscopy (FTIR), scanning electron microscopy (SEM), Brunauer–Emmett–Teller (BET) surface area analysis, and X-ray diffraction (XRD), along with measurements of pH, density, solubility, and proximate properties.

FTIR analysis of chemically activated carbon revealed O–H and C–H stretching vibrations, C–O bonds, and phosphate-related groups (P–O and P=O), indicating successful incorporation of functional groups from phosphoric acid. In contrast, the physically activated carbon showed C=C stretching and aromatic C–H bending vibrations. SEM images confirmed a more porous and tubular morphology for the chemically activated sample, while the physically activated carbon appeared denser with irregular granules. BET results showed higher surface area for chemical activation (678.01 m^2/g) than physical activation (455.22 m^2/g). Additionally, the chemically activated sample had higher fixed carbon (64.91%) and yield (24.2%), while the physically activated carbon showed higher pH (10.94) and density (0.94 g/cm^3). Both ACs achieved over 80% removal efficiency for methylene blue and methyl orange dyes, highlighting their effectiveness.

Thus, this research study will be of interest to water treatment utilities. Moreover, the research will contribute new knowledge and a better understanding of activated carbon from waste paper.

Keywords: Activated carbon, adsorption, chemical activation, physical activation, contaminants, removal efficiency.

List of Conference Proceedings:

1. Willemse V. C. P, Rahman A. & Kalili K., M. Activated carbon from Waste paper for the removal of methylene blue. 10th International Baskent Congress on physical, Engineering and Applied Sciences. Ankara, Turkey. 28-30 October 2023. (Presentation).

2. Willemse V. C. P, Rahman A. & Kalili K., M. Activated carbon from Waste paper for the removal of contaminants from wastewater. National Students' Research Symposium. 17-18th November 2023. (Presentation).

3. Willemse V. C. P, Rahman A. & Kalili K., M. Activated carbon from Waste paper for the removal of contaminants from wastewater. Chem4Energy Annual Conference. Materials and Processes for a Sustainable Energy Future. 7- 11 April 2025. (Presentation).

Table of Contents

List of Tables

List of Abbreviations and Acronyms

% ash	Percentage ash
% density	Percentage density
% moisture	Percentage moisture
% volatile matter	Percentage volatile matter
% yield	Percentage yield
AC	Activated carbon
BET	Brunauer-Emmett-Teller
BJH	Barrett-Joyner-Halenda
COD	Chemical oxygen demand
C_e	Equilibrium concentration
C_o	Initial concentration
FTIR	Fourier- Transform infrared spectroscopy
GWCW	Gammams Water Care Works
H_2O	Water
K_f	Adsorption capacity
MB	Methylene blue
MO	Methyl Orange
n	Freundlich constant
pH	Potential of hydrogen
R	Separation factor
R^2	Correlation coefficient
TDS	Total dissolved solid
UV/VIS	Ultraviolet/visible
WHO	World Health Organisation
XRD	X-ray diffraction

Acknowledgments

I extend my heartfelt gratitude to my supervisor, Prof. Ateeq Rahman, for his invaluable guidance, patience, and unwavering support throughout this research journey. Your encouragement and insightful advice continuously motivated me to give my very best—I will always remain grateful. A sincere thank you to Dr. Kalili for your kind assistance and contributions along the way.

I also wish to acknowledge the University of Namibia, particularly the Department of Physics, Chemistry, and Material Science, for providing access to the facilities and equipment that made this research possible.

To my dearest family- Mom, Dad, Vital, Vivalda, Rousie, Denise, and Abel- thank you for being my unwavering source of strength and love. Your constant support has meant the world to me.

To my amazing husband, Vincent Chanza, thank you for believing in me even when I doubted myself. Your endless encouragement and love lifted me through the most challenging moments. You've made me feel like I could conquer anything. To my mother-in-law, Christine Chanza, and abusa Juma thank you for always being my prayer warriors. Your spiritual support has been a powerful force behind me. I appreciate you both so much.

Lastly, I give thanks to Jehovah God for His divine protection and presence in my life. I have felt your guidance every step of the way.

Dedications

I dedicate this research to my anchor and guiding light, my mother, Fernanda Willemse. Your unwavering belief in me, especially during moments I doubted myself, has shaped me into the confident woman I am today. Thank you mama.

Declaration

I, **Viola-De-Amor C. P. Willemse**, hereby declare that this study is my own work and is a true reflection of my research and that this work, or any part thereof has not been submitted for a degree at any other institution.

Viola-De-Amor C. P. Willemse		31/10/ 25
Name of Student	**Signature**	**Date**

CHAPTER 1: INTRODUCTION

1.1 Background of the proposed study

Water sources are being contaminated by various sources such as industries, agricultural activities, pharmaceuticals and human activities [1-2]. The application of activated carbon in wastewater treatment is favourable due to high physicochemical stability, high porosity, high adsorption capacity, and large surface area [3-4]. Activated carbon from coconut shell, peat, hard and softwood, lignite coal, bituminous coal, olive pits, and various carbonaceous materials have been found effective in the removal of organic compounds, heavy metals, dyes, taste and odour from wastewater [5-6]. According to a report, nearly one-fifth of the contents of household dustbins consist of paper, which is equivalent to over 4 kg of waste paper per household each week [7]. In Namibia, about 33% of recyclable papers are disposed of at dumpsites and landfills with associated open burning [7]. Burning can lead to the release of hazardous substances such as CO_2 which is detrimental to the ozone layer. Recycling or finding alternative uses for waste paper would help to minimise burning and in turn reduce burning.

1.1 Statement of the problem

Sources of drinking water are subject to contamination and require appropriate treatment to remove contaminants. Climate change is severely exacerbating the water crisis hence it is prudent to search for ways in which contaminated water can be treated at a low cost. Equally important, the contamination of water from industries is gradually increasing and this accumulation will eventually exceed certain threshold concentrations and cause detrimental pollution. Furthermore, wastewater treatment

plants require various types of ACs in large quantities, and in Namibia, most treatment plants purchase ACs from abroad.

1.1 Objectives of the study

This study therefore aimed to prepare activated carbon from waste paper and evaluate its effectiveness in wastewater treatment. The specific objectives are:

- To prepare activated carbon from waste paper (copy paper) through physical activation as well as chemical activation, using H_3PO_4 as an impregnating agent.
- To characterise the prepared activated carbon by the following analytical instruments: Brunauer –Emmett Teller (BET), Scanning Electron Microscopy (SEM) and Fourier Transform Infrared Spectroscopy (FTIR) and X-Ray Diffraction (XRD) analysis.
- To evaluate the potential and effectiveness of activated carbon from waste paper for the removal of contaminants in wastewater.
- To compare the performance of the prepared activated carbons with industrial activated carbon for domestic wastewater treatment.

1.4 Significance of the study

Water is an essential resource for human life, as it has numerous uses in various sectors in Namibia such as agriculture, mining, domestic usage, industrial, power plants, and so forth. Since fresh water is in limited supply and the quality is under continuous strain, a series of studies need to be carried out. This study will provide knowledge and information on the use of activated carbon from waste paper (Copy paper) for wastewater treatment and give researchers an insight for further water treatment

studies. This means that academics, scholars, researchers, and water treatment facilities will be direct beneficiaries of this study. Furthermore, this study could be applied to large-scale use that can be piloted in Namibia.

1.5 Limitations of the study

In this study, only phosphoric acid was utilised as an impregnating agent for the chemical activation of activated carbon. Physicochemical tests were performed to assess water quality after using AC to treat contaminated water. No microbiological testing was performed. Furthermore, only wastewater from the Gammams Water Care Works (GWCW) was investigated in this study.

CHAPTER 2 : LITERATURE REVIEW

2.1 Water Treatment Methods

Water treatment involves the removal of impurities and contaminants, such as bacteria, minerals, sulfur, nitrogen, manganese, and other organic and inorganic substances. The specific treatment process is selected based on the type and concentration of contaminants [1]. Additionally, the choice of wastewater treatment methods depends on the degree of method required to bring the wastewater to a permissible level, the flexibility of the control method, the cost of the process, and the environmental compatibility [2]. There are various available methods of impurities removal from water, and they are categorized into chemical [3], physical [4], and biological [5] modes.

Several technologies, such as coagulation, flocculation, and advanced oxidation processes, have been tested for the removal of organic micropollutants. However, these advanced treatments still have numerous disadvantages, namely low removal rates for a large number of pharmaceuticals and/or the formation of by-products, causing a potential risk of contamination for treated water [6]. Oxidation processes show high efficiencies for the removal of contaminants, but the reaction is non-selective, so degradation of the molecules may cause the generation of undesired by-products, which may even be more toxic than the initial contaminant [7]. Other treatment methodologies such as membrane filtration, ion exchange, and reverse osmosis are expensive [6,7]. Sedimentation, filtration, and flocculation are frequently used only when physical particles must be removed [8]. All the above-mentioned methods have been efficient for contaminants removal, however, the adsorption method has been highly recommended by researchers in recent decades due to its advantages which

include being low cost, high efficiency, and environmentally friendly, ease of operation and low energy consumption [9].

Adsorption has a phase-changing mechanism in which the contaminants (adsorbates) move from the aqueous phase to the solid phase (adsorbent) and has been widely explored for the removal of impurities in wastewater treatment plants [10]. The adsorption efficiency depends on the properties of the impurities such as the molecular size, polarity, and functional group, and the adsorbent's properties such as the particle size, surface area, pore diameter, and environmental conditions (pH, temperature, wastewater type, etc) [10]. During the adsorption process, bond attraction forces, like van der Waals forces, trap the unwanted molecules within the activated carbon's internal pore structure and accumulate them onto a solid surface [1].

In this context, activated carbon (AC) is considered a highly efficient adsorbent due to its high surface area (S_{BET}) and interesting surface chemistry properties, showing high pharmaceutical removal rates [9]. Adsorbents play a significant role in the adsorption process, therefore selecting effective adsorbents is very important. Different types of adsorbents have been utilised for the adsorption process including activated carbon, graphene oxide, zeolite, clay and metal–organic frameworks [11,12].

Table 1: Wastewater Treatment Technologies

Type of treatment	**Advantages**	**Disadvantages**	**Reference**
Biological	Potential for removing metals	Technology is still under development	[13,14]
Photocatalysis	High degradation rate	Potential to be harmful to operators due to exposure to carcinogenic UV light.	[15]

Membrane technology	Membrane properties could be adjusted. High processing efficiency	Membrane fouling	[16]
Adsorption **(Research interest)**	Environmentally friendly, simple design, cost-effective and excellent for organic pollutants removal.	Requires regeneration of the adsorbent.	[17], [18], [19], [20], [21]
Coagulation/ flocculation	Simple process, good for reclamation to remove pollutants.	Require high dosage. Produce more sludge.	[22]

2.2 Activated carbon properties and structure

Activated carbon (AC) is a microporous form of carbon with a well-developed pore structure with functional groups on its surface, large pore volume, high internal surface area [1], and consequently, a high adsorption capacity [23]. The adsorption capacity of an activated carbon depends on its physical and chemical characteristics (pore size, functional groups) and the characteristics of the adsorbate (size, hydrophobicity) [24]. AC is highly used in industries due to its excellent mechanical properties, high porosity, high surface area, and the presence of organic/ inorganic functional groups [25]. These properties found in AC are influenced by the precursor and the mode of activation used in its preparation [26]. The activation process is key in the production of AC and, the shape and the size of pores in the AC are influenced by either chemical or physical activation [27]. The diversity of its precursor and different activation

processes could lead to the complexity and variety of its structure which results in different kinds of adsorption behaviour [28].

The carbon structure of AC is composed of different main functional groups such as phenol, carboxyl, lactone, carbonyl, and quinone [29]. The presence of functional groups on the surface of the activated carbon can affect the dispersion interactions between the aromatic rings of the graphene layers of activated carbons and the aromatic rings of the molecules and the presence of water can enhance or decrease the adsorption of organic molecules due to hydrogen bonding [30]. The main functional groups in the carbon structure of AC are responsible for the adsorption of pollutants [31] and the availability of oxygen, hydrogen, sulfur, and nitrogen can participate in the structure of AC in the form of functional groups or chemical atoms [31].

In recent years, researchers have used various agricultural wastes such as peach stones [32], date stones [33], plum kernels [34], peanut shells [35], orange peels (hydrochars) [36], rice husks [37] and corncob [37] as precursors of AC.

There are two major steps in producing AC. The first step is the carbonisation process, a thermal degradation process that occurs in the absence of oxygen [38]. At this step, the precursor is converted into char by subjecting it to a moderately high temperature between 400 and 600 °C and the main purpose of carbonisation is to increase the carbon content and to build the preliminary pores network [38]. Additionally, it reduces the volatile content of raw materials via pyrolysis of the carbon precursors in the temperature range of 300 – 900 °C and creates char with primary porosity associated with a high content of fixed carbon [38]. The next step is the activation process which can be physical activation, chemical activation, and physicochemical activation [37, 38]. The lower activation temperature allows more acidic functional

groups, including carboxyl, phenolic hydroxyl groups, and lactones, to be retained in the activated carbon, and phosphorus species can also be introduced to provide additional functional groups to further improve the adsorption of basic dyes [11]. The purpose of activation is to improve the specific surface area or pore volume of AC by opening new pores and developing the existing pores [37]. Activation is considered to be more crucial than carbonisation in terms of the properties of AC and it can vary or adjust the surface chemical nature of AC with certain unique characteristics [38].

Presently, physical activation, chemical activation, and physiochemical activation are the main activation techniques used [39], [40]. Physical activation is a dual-stage process, the raw material is pyrolysed at a higher temperature (600 –900 °C) in an inert atmosphere and then the carbonised material is exposed to the oxidising atmosphere (oxygen, carbon dioxide, or steam) at a higher temperature [1], in the temperature range of 800–1200 °C [37], [41]. In physical activation, the reactive carbon present in the adsorbent is eliminated and this followed by gasification resulting in the synthesis of the activated carbon with improved porosity [42]. Physical activation is clean and greener without any secondary waste disposals compared to chemical activation [43], [44]. The drawbacks of physical activation are related to its high activation temperature, considerably long processing time, relatively low carbon yield, and poor specific surface area [44].

Chemical activation is a process that involves the use of chemical agents to create micropores through dehydration and oxidation, during which carbonisation and activation take place simultaneously in the temperature range of 450 – 850 °C [38], for a better adsorbent surface area [45]. The advantages of chemical activation are its low heating temperature, short processing time, high carbon yield, well-controlled porosity, and high specific surface area [45]. However, the disadvantages of chemical

activation include its drastic corrosivity and inevitable washing process, and its dependence on the type of activating agent, mixing method, mass ratio of activating agent to carbon precursor, and heating method [46]. Many chemical reagents have been used as activating agents during the chemical activation process. In the chemical activation process, acids (such as H_3PO_4, H_2SO_4, and HNO_3), alkalis (NaOH and KOH), and $ZnCl_2$ are frequently used to decrease reaction temperatures and contact times [46]. In general, the modification of the AC surface has been mainly addressed in terms of oxidation, acidic or basic treatments [47].

Phosphoric acid, which is the chemical agent used in this study, is one of the most used activating agents due to its highly polar characteristics and it is believed that phosphoric acid promotes the formation of micropores inside the AC structure through forming phosphorus compounds and as a result, phosphoric acid interacts with the phenolic and carbonyl groups of the AC [44]. To add on, the generated substances such as phosphate would adhere to the surface of AC [48], protecting its internal structure. As a Brønsted acid, phosphoric acid can also catalyse the dehydration, condensation and aromatisation of aliphatic structures in biomass to form enriched porosity constructs [49,50]. Phosphoric acid has a lower activation temperature, higher carbon yield, and the production of structures that are predominantly mesoporous [11]. Moreover, phosphoric acid acts as a catalyst to adjust and control the textural properties of the AC by facilitating the carbon dioxide release from the inside of the AC structure and it has been proved that removal of volatile gas from the carbon structure will result in the formation of the regular pores in the side carbons [51].

2.3 Granular and powdered AC

The AC is marketed in two forms namely, granular activated carbons (GAC) and powdered activated carbons (PAC). GAC typically has particle sizes ranging from 200 to 5000 μm (0.2 mm to 5 mm), whereas PAC has much smaller particles, with sizes predominantly less than 100 μm [52]. The PAC usually exhibits high specific surface area and micro-porosity which increases their adsorption capacity [35]. PAC shows slower settling and removal tendencies than GAC [35]. Though PAC has a higher adsorption capacity, it can not be regenerated due to difficulties in separating it from the aqueous solution [35]. Because of these difficulties, PAC is mainly used in batch modes, especially in water treatment facilities [53]. GAC exhibits lower adsorption capacities for pollutant removal from aqueous solutions compared to PAC due to the fouling effect, as well as to the reduced mass transfer of the target pollutants [54]. The GAC is currently used as a water treatment material to effectively remove several pollutants including organic micropollutants, pharmaceuticals, arsenic, carcinogenic compounds, microplastics, heavy metals, colour, and odour [55]. The choice for GAC depends on the target pollutant, the concentration of the pollutant, flow rate, and adsorption capacity and these factors also influence the life span of the carbon [56].

Since the adsorbent capacity of GAC is limited, studies have been carried out to enhance its efficiency by modifying its structure with chemical agents [57]. Many investigations have shown that modified GAC enhances the adsorption of contaminants on its surface owing to chemosorption [57, 58]. A study used magnesium-modified granular AC and observed that the cadmium (II) removal capacity of the adsorbent increased from 3.47 to 8.48 % [58]. The uptake capacity of rice husks AC to remove lead (II) was increased after modification by nitric acid to

improve pore structure and surface functional groups like carboxyl and hydroxyl [58]. Steam-activated granular AC was previously used to treat wastewater of battery recycling unit and sulfuric acid was chosen as the modification agent to enhance the adsorption characteristics of the AC [58,59].

2.4 Waste paper recycling

Waste recycling has long been a critical environmental concern worldwide, particularly given its impact on resource conservation and energy efficiency. A study by Okada et al., [59] observed numerous studies underscore the importance of waste paper recycling, emphasising its role in conserving natural resources and reducing energy use [59]. Waste paper recycling, in particular, is recognised as a vital contributor to the long-term preservation of forest resources. Paper and cardboard account for approximately 10% of municipal solid waste [59,60], signifying a substantial opportunity for the reuse within the recycling stream. Transforming waste paper into AC offers a sustainable approach to paper waste management, with significant environmental and economic benefits. Due to the limited recyclability of cellulose fibers in waste paper, they often end up as disposal waste. However, by converting these fibers into AC, a material known for its high porosity and sorption capabilities, they can serve valuable applications in water purification, gas separation, and humidity control. Producing AC from waste paper typically involves both chemical and physical activation techniques. In a study by Okada et al., potassium carbonate (K_2CO_3) was used as a chemical activating agent to create AC with an impressive specific surface area of around 1700 m^2/g [59], enhancing its suitability for environmental uses such as methylene blue dye removal from water. Other agents, including Na_2CO_3, Li_2CO_3, and steam, have also been explored, producing variations in surface area and pore structure. These findings highlight waste paper-derived AC as

an effective, low-cost, and eco-friendly material, showcasing its potential as a sustainable solution for environmental protection.

2.5 Adsorbates of research interest

Research interest in treating pollutants such as Methyl Orange, Methylene Blue, and Copper Sulphate using activated carbon arises from their extensive use and significant environmental impact. Additionally, the Gammams Water Treatment Plant, a domestic wastewater treatment facility in Windhoek that utilizes activated carbon, is also a focus of study, highlighting the practical application of AC in wastewater treatment processes.

2.5.1 Methylene Blue

Methylene blue (MB) is a synthetic cationic dye extensively used in industrial and laboratory applications. While it serves various beneficial roles, MB also has potential environmental and health risks associated with its release [61,62]. On the positive side, MB is commonly used as a staining agent in medical diagnostics, a colourant in textile and paper industries [61], and a reagent in chemical laboratories [61], providing critical utility in these fields. However, when discharged into the environment, methylene blue becomes a persistent contaminant that can adversely affect aquatic ecosystems. The dye can impede the photosynthetic activities of aquatic plants, disrupt oxygen production, and harm aquatic organisms, ultimately impacting the biodiversity of affected ecosystems. Due to its resistance to natural degradation, MB's presence in water bodies is a growing environmental concern [62].

2.5.2 Methyl Orange

Methyl orange (MO), an anionic dye widely used in laboratories and industrial processes, is particularly known for its role as a pH indicator in titrations and as a colorant in textile and leather industries [63]. Despite its value in analytical and industrial applications, methyl orange poses environmental and health risks. When released into natural water bodies, it can harm aquatic ecosystems by interfering with photosynthesis in aquatic plants and altering the ecological balance, which can reduce biodiversity [30, 63,64]. In addition, MO poses potential health risks to humans, especially when found in high concentrations, as it may cause skin and eye irritation, with concerns over its possible carcinogenicity. These hazards underline the importance of managing and minimizing MO discharge in wastewater [64].

2.5.3 Copper Sulphate

Copper sulphate ($CuSO_4$) is a widely used compound in various sectors, including agriculture, industrial manufacturing, and as an algicide [65]. However, it presents significant risks to both the environment and public health if not carefully managed. Copper, when introduced into aquatic systems, can be toxic to fish, affecting gill function and disrupting essential enzymatic processes [65,66]. For humans, prolonged exposure to copper through contaminated water or food sources can lead to gastrointestinal issues, liver damage, and kidney disease. Copper's persistence as a heavy metal also allows it to bioaccumulate in living organisms, entering the food chain and posing chronic health risks. As such, it is crucial to regulate copper levels in wastewater, with adsorption techniques, such as using activated carbon, proving effective for copper removal in water treatment applications [66].

2.5.4 Gammams Water Care Works

The Gammams Water Care Works (GWCW) is a primary domestic wastewater treatment facility located in Windhoek, Namibia. Wastewater samples for analysis were obtained from this facility, which processes wastewater from surrounding residential suburbs. Samples were collected from two critical points: the influent, or raw water entering the facility, and the effluent, the semi-treated water which undergoes further purification at the Windhoek Goreangab Operating Company (WINGOC). These sample points allow for analysis of the treatment stages and effectiveness of the GWCW in reducing pollutants before final discharge or further treatment.

2.6 Water Quality Testing Parameters

The decline in global water quality has become a significant concern, largely due to the cumulative impact of industrial and agricultural activities [67,68]. According to UN-Water (2022), urgent attention and intervention are essential to address water quality issues, as these problems are complex and multifaceted. Both human activities and natural processes contribute to the complexity of water quality in groundwater and surface water, making comprehensive testing crucial before water is used for domestic, industrial, agricultural, or drinking purposes [69]. Poor water quality can have severe consequences, not only for aquatic life but also for the surrounding ecosystems. Routine monitoring allows researchers to understand natural environmental processes and assess the extent of human impact on ecosystems. Water quality testing involves analysing several physio-chemical parameters, chosen based on the intended water use and specific purity requirements [68]. Water contains various dissolved, suspended, and bacteriological impurities that demand careful assessment.

The physical properties of the wastewater were evaluated by measuring total dissolved solids (TDS) and turbidity, while chemical parameters were assessed through tests for conductivity, salinity, and dissolved oxygen. The World Health Organisation (WHO) provides recommended guidelines for these parameters to safeguard human health and the environment [70]. In Namibia, water quality standards for drinking water are set by the Ministry of Agriculture, Water and Forestry, and the Ministry of Health and Social Services, following WHO guidelines but with modifications by local researchers and expertise [67].

The following water quality parameters discussed below are executed in this research.

2.6.1 Total Dissolved Solids

The World Health Organization (WHO) indicates that the palatability of water is generally deemed satisfactory when the concentration of Total Dissolved Solids (TDS) is below 600 mg/L. Conversely, TDS levels exceeding 1000 mg/L can significantly detract from the taste and overall acceptability of the water, rendering it unpalatable to consumers. High concentrations of TDS can lead to extensive scaling in water delivery systems, such as pipelines, heaters, and boilers, as well as in various household appliances, which can further diminish the overall user experience. Notably, there is currently no established guideline for TDS levels that directly correlates with health impacts, making it essential to consider TDS levels in the context of water quality management.

2.6.2 Dissolved Oxygen

Dissolved oxygen (DO) is an essential water quality metric that is crucial for evaluating the health and overall integrity of aquatic ecosystems. The concentration of dissolved oxygen in a body of water serves as a vital indicator of its capacity to sustain

aquatic life, particularly fish and other organisms that depend on oxygen for survival. A sufficient level of dissolved oxygen typically signifies good water quality and a healthy ecosystem. In contrast, low dissolved oxygen levels may signal the presence of pollution, the breakdown of organic matter, or other conditions that could disrupt the ecological balance within the water body [67]. Therefore, monitoring DO levels is fundamental for the conservation of aquatic environments.

2.6.3 Conductivity

Conductivity is a significant indicator of water quality, quantifying the ability of water to conduct an electric current [68]. This measurement is largely influenced by the concentration of dissolved ions present in the water. Conductivity serves as a crucial indicator of various aspects of water quality, as it can quickly reveal changes in pollutant concentrations, including nutrients, heavy metals, and industrial effluents. An increase in conductivity often suggests potential contamination, which can enable early detection and timely intervention to mitigate negative environmental impacts before they escalate into more serious issues [69].

2.6.4 Turbidity

The turbidity of water is caused by the presence of colloidal or suspended particles that obstruct the passage of light through the liquid. These particles are attributed to a variety of sources, including both organic and inorganic materials, or a mixture of the two. Since bacteria, viruses, and protozoa frequently attach themselves to these particles, implementing effective filtration systems becomes vital. Filtration not only eliminates turbidity but also plays a key role in reducing microbial contamination in treated water, as emphasized by the WHO in 2011 [70]. In certain groundwater sources, turbidity may arise from the presence of chalk particles, the precipitation of

insoluble forms of reduced iron, inert clay, or other oxides, particularly when water is extracted from anaerobic environments. Moreover, turbidity can significantly hinder the effectiveness of disinfection processes by providing shelter for microorganisms. Consequently, a considerable portion of water treatment efforts focuses on the removal of particulate matter prior to disinfection. Turbidity is measured in Nephelometric Turbidity Units (NTU), with turbidity that is visibly detectable by the naked eye usually recorded above approximately 4.0 NTU, according to WHO standards in 2011 [70]. For effective disinfection, however, it is ideal that turbidity levels remain below 1 NTU, and it is preferable for them to be much lower than that threshold [70].

2.6.5 Salinity

Salinity is a fundamental water quality metric that plays a vital role in the comprehension and management of aquatic ecosystems. It quantifies the concentration of dissolved salts in water, with sodium chloride being the predominant component [68,69]. The salinity levels within water bodies have significant implications for the distribution, behavior, and health of various aquatic organisms. Different species of fish, invertebrates, and plants possess specific salinity tolerance ranges; deviations from these ranges can lead to stress, health issues, or even mortality among these organisms. Additionally, monitoring salinity is crucial in agricultural contexts, as high salinity levels in irrigation water can adversely affect soil structure and crop health [68]. Overall, salinity serves as a critical diagnostic tool for assessing the suitability of water for multiple uses, enhancing our understanding of ecosystem dynamics, and enabling the implementation of effective management strategies aimed at preserving the health and balance of aquatic environments.

2.7 Adsorption isotherms

Adsorption isotherms play a pivotal role in water treatment processes, serving as a fundamental tool to understand and optimise the adsorption of contaminants onto solid surfaces [71]. In the realm of water purification, the relationship between the concentration of pollutants in the liquid phase and their uptake onto the adsorbent material is crucial for designing efficient treatment systems. Various isotherm models, such as the Langmuir and Freundlich equations, offer insights into the adsorption capacity, surface coverage, and affinity of adsorbents for specific contaminants. These isotherms help engineers and researchers predict the equilibrium behaviour of adsorption systems, facilitating the selection and optimisation of adsorbents for water treatment applications [72,73]. By harnessing the principles of adsorption isotherms, water treatment technologies can be tailored to remove pollutants efficiently and sustainably, ensuring the delivery of clean and safe water for diverse purposes. This research employed the two adsorption isotherms, the Langmuir and Freundlich isotherms, and these are discussed briefly below.

2.7.1 Langmuir adsorption isotherm

The Langmuir adsorption isotherm is a fundamental model that describes the relationship between the adsorption of the adsorbate and adsorbent [72]. This model is particularly applicable to monolayer adsorption on a homogeneous surface, assuming that once a site on the adsorbent surface is occupied, no further adsorption can occur at that site.

The Langmuir isotherm is based on the following assumptions [73]:

1. Adsorption occurs at specific homogeneous sites on the adsorbent surface.
2. Each site can only accommodate one adsorbate molecule.
3. All adsorption sites are equivalent and energetically identical.
4. No interaction occurs between adsorbate molecules once they are absorbed.

The Langmuir adsorption isotherm is widely used in the analysis of adsorption data and provides valuable information about the maximum adsorption capacity and the affinity of an adsorbate for a specific adsorbent under idealised conditions [74]. It serves as a foundational model in understanding and predicting adsorption behavior in various practical applications, such as in the design of water treatment processes or the development of adsorption-based technologies.

2.7.2 Freundlich adsorption isotherms

The Freundlich adsorption isotherm is a widely used model that describes the relationship between the adsorption of a solute onto a surface and its concentration in the solution at equilibrium. Unlike the Langmuir isotherm, the Freundlich model does not assume monolayer adsorption but allows for the formation of multilayer adsorption on a heterogeneous surface [72, 75]. The Freundlich isotherm is particularly suitable for describing adsorption on surfaces with varying affinities or energies. The Freundlich adsorption isotherm is versatile and can describe a range of adsorption behaviours, making it applicable to a variety of adsorption systems [75].

2.8 Effects of parameters on adsorption efficiency

2.8.1 Effect of Initial Concentration

The initial concentration of a solute in the solution significantly affects the adsorption process by influencing the driving force that propels solute molecules onto the surface of the adsorbent material. When the starting concentration of a contaminant is higher,

a larger concentration gradient exists, which intensifies the mass transfer rate of solute molecules toward the adsorbent's surface, leading to a stronger driving force for adsorption [60]. This enhanced concentration gradient often results in a quicker and more efficient adsorption process, as it promotes rapid movement and attachment of contaminants to the adsorbent. Investigating the effect of initial concentration provides researchers with critical insights into the adsorption capacity and potential efficiency of activated carbon in removing contaminants. Furthermore, understanding how varying initial concentrations impact equilibrium adsorption capacity aids in optimizing the design and operational parameters of adsorption systems for real-world applications, such as wastewater treatment or pollution control. Such knowledge is invaluable for ensuring that adsorbent materials are applied most effectively in addressing environmental contamination challenges.

2.8.2 Effect of Time

Time is a crucial parameter in batch adsorption studies, directly affecting both the kinetics and the equilibrium state of adsorption. Studying the time variable in adsorption experiments reveals the dynamics of interaction between the adsorbate (the material being removed) and the adsorbent surface, helping researchers understand the rate at which the adsorbate attaches to the adsorbent over time [61,62]. Observing adsorption over time allows scientists to track trends and determine the point at which the adsorbent reaches its saturation capacity, signifying the optimal contact time necessary for achieving the maximum adsorption potential of the material [63]. Such time-related observations help establish when the adsorption system reaches equilibrium and can no longer increase its capacity for adsorbing contaminants, which is essential for planning efficient batch processes. By identifying the ideal contact time, adsorption systems can be fine-tuned to minimize resource use and maximize

effectiveness, ultimately enhancing the feasibility of these systems for large-scale water treatment or pollutant removal applications.

2.8.3 Effect of Temperature

Temperature is a critical factor in adsorption studies, as changes in temperature can significantly influence the rate of adsorption and the equilibrium capacity of an adsorbent. Variations in temperature affect the energy levels of both the adsorbent and adsorbate, altering the strength of interactions between them and providing insight into the exothermic or endothermic nature of the adsorption reaction [64]. Through temperature analysis, researchers can determine the conditions under which the adsorbent material performs most efficiently, enabling the optimization of adsorption systems for specific uses. In real-world applications, such as wastewater treatment, temperature adjustments may be needed to enhance adsorption capacity and ensure stable performance under diverse environmental conditions. Temperature studies are therefore indispensable for developing adaptable and effective adsorption systems, allowing them to achieve consistent contaminant removal and maintain efficiency even when exposed to varying external conditions.

2.8.4 Effect of Adsorbent Dosage

The amount of adsorbent material added to a solution is a crucial parameter that impacts the available surface area for adsorption and, by extension, the capacity for contaminant removal. Determining the appropriate adsorbent dosage is essential to strike a balance between maximizing adsorption efficiency and minimizing costs associated with excess material use [65]. An insufficient adsorbent amount may result in partial or incomplete contaminant removal, while an excessive amount may lead to diminishing returns without a proportionate increase in adsorption capacity. By

systematically adjusting adsorbent dosages, researchers can establish the ideal amount of material needed to achieve maximum contaminant adsorption while maintaining cost-effectiveness. Optimizing adsorbent dosage is a key step toward developing sustainable, resource-efficient adsorption systems that are economically viable for environmental cleanup applications [65,66]. This knowledge contributes to more efficient contaminant removal processes and supports the practical implementation of adsorption technologies for a range of pollution control and treatment scenarios.

2.8.5 Effect of pH

The pH level of a solution plays a vital role in the adsorption process, as it influences both the charge characteristics of the adsorbent material and the ionization state of the adsorbate. These factors determine the degree and nature of electrostatic interactions between the adsorbent and adsorbate, impacting the efficiency of adsorption [67]. Changes in pH can alter the surface charge of the adsorbent, thereby affecting its affinity for charged contaminants in the solution. By examining how different pH levels influence adsorption, researchers can identify the optimal pH range in which the adsorbent demonstrates the highest efficiency in removing target pollutants. This is particularly important for environmental applications, such as water purification, where the pH of source water can vary and affect contaminant removal. Studying the effect of pH in batch adsorption experiments allows researchers to design and adapt adsorption systems for specific environmental conditions, enhancing their applicability in diverse settings. This comprehensive understanding ensures that adsorption technologies can be tailored to maintain high performance and reliability in removing contaminants, thereby contributing to effective water treatment and pollutant mitigation strategies [68].

CHAPTER 3: RESEARCH METHODS

3.1 Materials and Chemicals used

Chemicals including phosphoric acid, copper sulphate, hydrochloric acid, sodium hydroxide, sodium silicate, oleic acid, activated carbon, methyl orange, and methylene blue were procured from Sigma Aldrich. Filtration procedures employed a Diaphragm vacuum pump (model D97877), alongside Whatman® ashless filter papers (125 mm). Purified water was sourced from a Millipore Integral 3 water purification system.

3.2 Instrumentation

All carbonisation and activation tests were performed using a muffle furnace. Water quality parameters- including dissolved oxygen (DO), salinity, conductivity, total dissolved solids (TDS), and pH- were measured using a multi-parameter meter (model HI982911042) from Hanna Instruments. Turbidity levels in each water sample were determined with the HACH 2100AN Laboratory Turbidimeter, following the AWWA/APHA: 2130 B Nephelometric Method. Cu^{2+} and dye absorbance measurements were carried out with a UV/Vis spectrophotometer (model DR6000 by Hach®), operating across wavelengths of 300 to 750 nm. Infrared (IR) analysis was conducted with a PerkinElmer Spectrum Two LITA Fourier Transform infrared spectrometer, covering the spectral range of 4000–400 cm^{-1} and utilising PerkinElmer Spectrum software (Version 10.5.1). Scanning electron microscopy (SEM) was performed using a JSM-IT300 microscope, with an accelerating voltage range of 0.3 kV to 30 kV. X-ray diffraction (XRD) analyses employed a Panalytical Aeris X-ray diffractometer, scanning from 5 to 80° 2-theta with a step size of 0.022° and a cobalt radiation source. For Brunauer–Emmett–Teller (BET) surface area analysis, the Tristar II 3020 version 3.02 with nitrogen adsorption was used.

3.3 Waste paper Collection and Preparation of solutions

Waste copy papers were collected around the University of Namibia (UNAM), while wastewater samples were sourced from the Gammams Water Care Works (GWCW) facility in Windhoek. These water samples were then transported to UNAM for treatment. The GWCW, located about 7 km north of central Windhoek in the Wanaheda suburb, serves as the municipal wastewater treatment plant for the city. Wastewater samples were specifically taken from both the inlet (influent) and outlet (effluent) stages of the treatment process. Additionally, dyes such as methylene blue (MB) and methyl orange (MO), along with the inorganic compound copper sulphate, were prepared in the laboratory at varying concentrations from 25 to 150 mg/L.

3.4 Deinking of Copy paper

The deinking of copy paper involved several key steps: pulping, blending, washing, and flotation. To remove ink from the paper, 50 g of copy paper was combined with 100 mL of 1% NaOH and 100 mL of 1% Na_2SiO_3, creating a pulp with a pH ranging from 12.1 to 12.58 [76]. The pulp then underwent flotation, where 50 mL of oleic acid (a foaming agent) and 5 L of distilled water were added. Air was bubbled through the pulp, causing hydrophobic molecules, like ink, to attach to the bubbles and separate from the mixture [77]. The deinked paper was then rinsed with warm distilled water to neutralise the pH and filtered using suction filtration to remove excess water. Finally, the paper was dried in an oven at 50° C overnight, after which it was blended and prepared for conversion into activated carbon through chemical and physical activation methods.

3.5 Preparation of Activated carbon

3.5.1 Chemical Activation

A 5% solution of phosphoric acid (H_3PO_4) served as the impregnating agent for the activation process. The acid was thoroughly mixed with deinked paper pulp, and the mixture was allowed to sit at room temperature for 24 hours to ensure optimal interaction between the acid and paper fibers. After this soaking period, the mixture was heated to 110 °C on a hot plate for two hours, facilitating further absorption. Next, the treated sample underwent suction filtration and was rinsed with warm deionised water until a neutral pH was achieved [61]. The sample was then dried overnight in an oven set to 110 °C. Once dry, the paper was finely blended, placed in crucibles, and subjected to a high-temperature treatment in a furnace at 600 °C for two hours to initiate the carbonisation and activation phases. After cooling to room temperature, the resulting activated material was washed with a 0.1% HCl solution (prepared by diluting 10 mL of concentrated HCl in 100 mL of distilled water) to eliminate any remaining impurities. This was followed by a second rinse with hot deionized water to ensure a neutral pH was maintained. Finally, the activated carbon sample was dried again at 110 °C overnight, then ground into a fine powder using a mortar and pestle. The finished activated carbon was stored in clean, airtight vials, ready for applications and further experimental use.

3.5.2 Physical activation

The de-inked waste copy paper was placed in crucibles and subjected to activation in a furnace set at 600°C for a duration of 2 hours. After activation, the samples were gradually allowed to cool to room temperature. The resulting activated carbon (AC)

was then thoroughly washed with a 0.1% HCl solution to eliminate any residual impurities, followed by rinsing with hot deionised water to achieve a neutral pH level [61,62]. Subsequently, the samples were dried in an oven at 110°C overnight to ensure complete moisture removal. Once fully dried, the activated carbon samples were grounded and carefully transferred to labelled vials for storage and ready for applications.

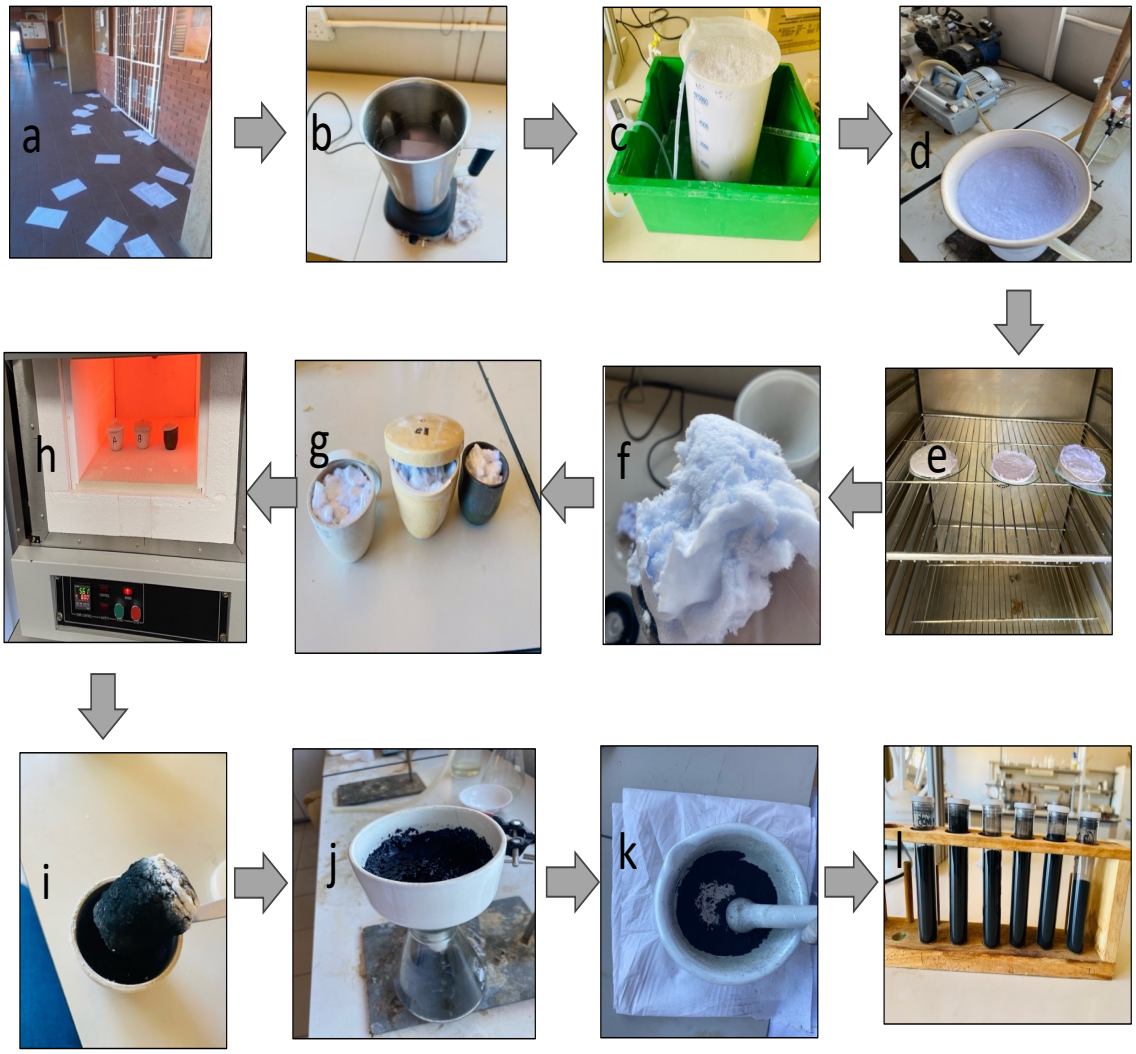

Figure 1 Research design: (a) Collection of waste copy paper; (b) Blending of copy paper; (c) Use of a flotation system to remove ink; (d) Washing and filtration of copy paper via suction; (e) Drying of copy paper in an oven; (f) Blended copy paper; (g) Placement of copy paper in crucibles; (h) Carbonization of activated carbon in a muffle furnace at 600°C; (i) Activated carbon prepared; (j) Washing of AC with 0.1%

HCl followed by distilled water; (k) Mechanical grinding of AC with mortar and pestle; (l) AC stored in vials, ready for application.

3.6 Characterisation of prepared Activated Carbon from waste paper

3.6.1 Physical Characterisation of Prepared Activated Carbon

3.6.1.1 Yield of cellulose Activated carbon

The percentage yield of each sample was determined by using the following equation [61]:

$$\% \text{ yield} = \frac{M_2}{M_1} \times 100 \qquad \textit{Equation 3.1}$$

where M_1 represents the mass (g) of copy paper and M_2 represents AC mass (g)

3.6.1.2 pH of Activated Carbon

0.5 g of the prepared ACs were placed in labelled 250 mL round bottom flasks. 100 mL of distilled water was added into the flask using a measuring cylinder. The mixture was stirred on a magnetic stirrer for 1 hour. A pH meter was used to determine the pH of the solutions and recorded.

3.6.1.3 H_2O Solubility of Activated Carbon

In a flask, 0.5 g of AC was added, then 25 mL of water was added. The flask was then connected to the condenser. Subsequently, the setup was brought to a boil on the hot plate and refluxed for one hour. Afterwards, the solution underwent filtration, and the resulting filtrate was transferred to an evaporating dish, weighed, and then placed on the hot plate for evaporation, followed by further drying in the oven. Once the solution

cooled to room temperature, it was weighed again. The water solubility was calculated as follows .

$$\%\ H_2O\ \text{Solubility} = \frac{W_1 - W_2}{W_1} \times 100 \qquad \textit{Equation 3.2}$$

where W_1 represents the mass (in grams) of the evaporating dish and water soluble and W_2 represents the mass of the empty dish (g)

3.6.1.4 Acid Solubility of Activated Carbon

In a flask, 0.5 g of AC was introduced, and 25 mL of water was added. Subsequently, 5 mL of concentrated HCl was introduced. The flask was then connected to a condenser. Following this, the setup was brought to a boil on the hot plate and refluxed for one hour. After the reflux, the solution underwent filtration, and the resultant filtrate was transferred to an evaporating dish, weighed, and placed on the hot plate for evaporation, followed by additional drying in the oven. Once the solution had cooled to room temperature, it underwent another weighing .

$$\%\ \text{Acid Solubility} = \frac{W_1 - W_2}{W_1} \times 100 \qquad \textit{Equation 3.3}$$

where W_1 represents the mass in grams of the evaporating dish and acid soluble and W_2 represents the mass of the empty dish (g)

3.6.1.5 Density of Activated Carbon

The densities of the prepared ACs were determined using a method similar to that of Guellati et al [55]. 0.5g of each AC was added to a 10 mL measuring cylinder and the volume readings were taken. The cylinders were tapped on a palm for 25, 50,75, and

100 times, and volume readings and masses were taken. The density was calculated using the formula:

$$\text{Density} = \frac{\text{mass of AC}}{\text{volume of AC}} \qquad \textit{Equation 3.4}$$

3.6.1.6 Moisture of Activated Carbon

The moisture content was determined by heating 0.5 g (W_1) of each sample and heating it in the oven for 2 hours at a constant temperature of 110°C [56]. The product was cooled at room temperature and reweighed (W_2). The moisture content for each sample was obtained using this equation:

$$\%\ \text{moisture} = \frac{W_1 - W_2}{W_1} \times 100 \qquad \textit{Equation 3.5}$$

3.6.1.7 Volatile matter

The volatile matter for each sample was determined by heating the crucible in the furnace for 1 hour at 650 ° C and weighed [78]. 0.5 grams (W_1) of the dry sample was added to the crucibles and weighed. The samples were heated in the furnace for 10 minutes at 900 ° C [78]. They were cooled in the desiccator and their masses (W_3) were taken after. The amount of the volatile matters in each crucible were determined by using the equation:

$$\%\ \text{Volatile matter} = \frac{W_1 - W_3}{W_1} \times 100 \qquad \textit{Equation 3.6}$$

3.6.1.8 Ash content

The ash content was determined by pre-heating three crucibles in a muffle furnace at 650 ^{o}C for 1 hour, cooling them in a desiccator, and weighing them [79] One gram(W_1) of each AC was added to the pre-weighed crucibles. These crucibles with AC were

placed in a muffle furnace and heated at 750 °C for 5 hours [79]. The crucibles were left to cool overnight and removed the following day and reweighed (W_2). The ash content for each sample was determined using equation:

$$\% \text{ ash} = \frac{W_2}{W_1} \times 100 \qquad \textit{Equation 3.7}$$

3.6.1.9 Fixed Carbon

Fixed carbon refers to the portion of solid carbon in biomass that stays within the char after the volatile components are removed during the pyrolysis process . It is calculated using the following equation [80]:

Fixed Carbon = 100 – (% moisture content+ % volatile matter + % ash content) *Equation 3.8*

3.6.2 Chemical Characterisation of Activated Carbon

3.6.2.1 Fourier Transform Infrared Spectroscopy Analysis

A small quantity of the activated carbon sample was placed on the sample holder, and infrared radiation was passed through it. The absorbance spectrum was recorded over a wavenumber of 4000–400 cm^{-1}. The resulting peaks were analysed to identify the functional groups present on the surface of the activated carbon, indicating chemical bonds and surface functionalities [58,59].

3.6.2.2 Scanning Electron Microscope

Activated carbon samples were mounted on stubs and coated with a thin conductive layer. The sample surface was then scanned with a focused electron beam. The emitted signals were collected to produce high-resolution images showing the surface morphology, including pore structure, shape, and distribution [59].

3.6.2.3 X-Ray Diffraction

Activated carbon samples were spread evenly on a sample holder and scanned using X-ray radiation over a range of angles. The diffraction pattern was recorded, and the positions and intensities of the peaks were analyzed to determine whether the activated carbon structure was crystalline or amorphous.

3.6.2.4 Surface area and porosity using the Brunauer-Emmett-Teller Analysis

In this study, nitrogen adsorption analysis was performed to determine the specific surface area, pore size and pore volume of the activated carbon produced from waste paper. The data were interpreted using the Brunauer-Emmett-Teller Analysis.

3.7 Evaluation of the effectiveness of the AC in removing contaminants in Wastewater

Batch adsorption experiments were carried out to examine the removal of dyes and Inorganic compound using the following parameters: pH (2 - 12), temperature (28.0 - 80.0°C), contact time (10 - 120 min), initial concentration (25 - 150 mg/L) and adsorbent particle size (0.05 - 0.2 g). The samples were analysed using the UV-Vis spectrophotometer, which showed the absorbance capacity of the ACs produced.

3.8 Adsorption Capacity of Prepared Activated carbon

To assess the adsorption capacity of the ACs, solutions of $CuSO_4$, MB and MO were utilised as adsorbates. It is to be noted that Cu^{2+} ions released from the dissociation of $CuSO_4$ in water was the focus of the study. Initially, stock solutions of $CuSO_4$, MB and MO were prepared with a concentration of 200 mg/L. Achieving solution homogeneity was ensured by stirring the solutions overnight with a magnetic stirring

bar. Subsequently, these solutions were appropriately diluted to create four distinct concentrations (25, 50, 100, and 150 mg/L for each compound), achieved by diluting 12.5, 25, 50, and 75 mL of the respective stock solutions in 100 mL of distilled water. To investigate the impact of different concentrations of MB and MO, 25 mL of various concentrations of each compound were placed in separate Erlenmeyer flasks, and 0.05 g of ACs were added to each flask. The solutions were gently stirred at room temperature (28.0 ° C) for 60 minutes. To examine the effect of time, 25 mL volumes of 100 mg/L concentrations of $CuSO_4$, MB and MO were placed in separate Erlenmeyer flasks, and 0.05 g of AC was added to each flask. The solutions were stirred at room temperature for various times (10, 30, 60 and 120 minutes). To study the effect of temperature, 0.05 g of ACs were placed in different flasks with 25 mL of 100 mg/L of $CuSO_4$, MB and MO, respectively. These flasks were subjected to various temperatures (28.0, 40, 60, and 80 ^oC) and stirred for 60 minutes. Finally, to examine the influence of pH, Erlenmeyer flasks containing 25 mL volumes of 100 mg/L concentrations of $CuSO_4$, MB and MO were prepared. To each solution, 0.05 g of AC was added. The pH levels were then adjusted to 2, 4, 8, and 12 using 0.1 M solutions of HCl and NaOH. Subsequently, the solutions were stirred at room temperature for 60 minutes.

Following the adsorption procedures, the samples underwent filtration, and the UV/Vis spectrophotometer was employed to measure the absorbance of $CuSO_4$, MO and MB. The concentrations and absorbances of the adsorbates were deduced from the calibration plot. The adsorbed quantities of Cu^{2+}, MO and MB by the prepared AC were expressed as removal percentages.

Removal efficiency was calculated using the following equation [80]:

$$\text{Removal Efficiency} = \frac{Intial\ Absorbance - Final\ Absorbance}{Intial\ Absorbance} \times 100 \qquad \textit{Equation 3.9}$$

3.9 Wastewater treatment with the prepared Activated carbon

Initially, the wastewater from the Gammams Water Care works facility (influent and effluent) underwent a 24-hour settling period without disturbance to facilitate the sedimentation of larger particulate impurities. The resulting decant was then filtered to remove suspended particulate matter that could potentially impede active adsorption sites on the activated carbon.

In 250 mL flasks, 100 mL of the clarified wastewater was placed. To evaluate the impact of adsorbent dosage, varying quantities of ACs (0.05, 0.1 and 0.2 g) were added to individual flasks. The solutions were gently stirred at room temperature for 60 minutes. Afterwards, water quality parameters, including conductivity, DO, turbidity, salinity, and TDS, were measured using a multi-parameter meter.

The influence of contact time on the treatment process was explored by introducing 0.1 g of AC into 100 mL of wastewater within a flask. Water quality parameters were then measured at different time intervals, specifically at 10, 30, 60 and 120 minutes. Lastly, the effect of temperature was assessed by subjecting the wastewater to various temperatures (28.0, 40.0, 60.0, and 90.0 ^{o}C) for 60 minutes with continuous stirring. 0.1 g of AC was used. This rigorous methodology allowed for the evaluation of the ACs efficiency in treating wastewater, considering adsorbent dosage, temperature, and contact time as crucial factors in achieving optimal purification outcomes.

3.10 Statistical Analysis:

Each experiment was conducted three times to ensure rigour, reliability, and the generation of meaningful conclusions, and the average results were used. The standard deviation of the averages was below 5, which indicates that the individual values used to calculate the averages are relatively close to the mean.

CHAPTER 4: RESULTS AND DISCUSSIONS

This chapter presents the results of the prepared activated carbon, focusing on both its physical and chemical characterisation. It evaluates the efficiency of the activated carbon in removing contaminants from domestic wastewater, as well as its effectiveness in adsorbing dyes (methyl orange and methylene blue) and copper ions (Cu^{2+}), which were introduced into solution through the dissociation of copper sulphate ($CuSO_4$). For clarity, AC-1 refers to activated carbon produced through physical activation, AC-2 refers to chemically activated carbon using phosphoric acid, and AC-3 represents commercial activated carbon.

4.1 Physical Characteristics of prepared Activated Carbon

Figures 2 – 4 summarizes the physical characteristics of three types of activated carbons: AC-1, AC-2, and AC-3. These parameters offer insights into the quality and suitability of each type of activated carbons.

4.1.1 pH

AC-1 exhibited the highest pH value of 10.94, indicating a strongly basic nature. This can be attributed to the presence of residual inorganic compounds such as mineral ash, which are often retained during physical activation. AC-2 showed a slightly alkaline pH of 8.27 due to the introduction of acidic phosphate functional groups from the phosphoric acid used during activation. These acidic groups partially neutralise the basic surface [11, 62]. AC-3 had the lowest pH (7.33). The pH values suggest that AC-1 may be more effective for adsorbing acidic pollutants, while AC-2 and AC-3 are better suited for use in neutral or slightly alkaline environments.

4.1.2 Density

AC-1 and AC-2 had relatively lower densities of 1.12 g/cm³ and 0.89 g/cm³, respectively, while AC-3 had the highest density at 1.80 g/cm³. The high density of AC-3 implies a more compact and uniform structure, characteristic of commercial activated carbons with controlled production processes [19, 25]. In contrast, the lower density in AC-2 suggests a more porous structure, which may enhance surface area and adsorption potential.

4.1.3 Yield of activated carbon

The carbon yield was highest in AC-2 (24.2%), followed by AC-1 (12.8%). This significant difference highlights the efficiency of chemical activation in preserving more carbon mass during production. Chemical agents such as phosphoric acid promote better structural retention, whereas physical activation often leads to greater mass loss due to higher thermal degradation [61].

4.1.4 Ash content

Ash content was highest in AC-1 at 16.7%, slightly lower in AC-2 at 14.29%, and completely absent in AC-3. High ash content indicates the presence of inorganic residues, which may block active sites and reduce adsorption efficiency [87,88]. The absence of ash in AC-3 points to a purer form of carbon, enhancing its effectiveness in adsorption applications.

4.1.5 Moisture content

Moisture content were highest in AC-1 (8.5%), followed by AC-2 (6.5%), with AC-3 having the lowest (0.17%). Lower moisture content is desirable, as excess water can hinder adsorption by occupying active sites [11, 88].

4.1.6 Volatile matter

Volatile matter, which reflects the presence of unstable organic compounds, was significantly higher in AC-1 (33.3%) compared to AC-2 (14.3%) and AC-3 (10%). Lower volatile content in AC-2 and AC-3 suggests a higher degree of carbonisation, enhancing their thermal stability and adsorption durability [88].

4.1.7 Fixed carbon

Fixed carbon is a key indicator of the quality and stability of activated carbon, as it reflects the amount of carbon available for adsorption and structural integrity. It was highest in AC-3 (89.83%), followed by AC-2 (64.91%) and AC-1 (41.5%). This pattern aligns with the greater thermal processing and activation efficiency of commercial and chemically activated carbons. Higher fixed carbon is preferred for better adsorption and thermal stability [26,88].

4.1.8 Acid solubility

Acid solubility tests help determine the stability of activated carbon in acidic environments and indicate the presence of acid-soluble impurities such as metal oxides or mineral residues. Among the samples, only AC-1 showed a 5% solubility in acid, while AC-2 and AC-3 were completely insoluble. The partial solubility of AC-1 is likely due to residual inorganic compounds left behind during the physical activation process, which are more prone to dissolution in acidic media. In contrast, the absence of acid solubility in AC-2 and AC-3 suggests that these carbons have a more stable and chemically resistant structure [27].

4.1.9 Water solubility

Water solubility was consistent across all samples (5%), indicating the presence of some water-soluble surface compounds or functional groups. These could include polar organic residues or loosely bound minerals that were not completely removed during washing [27]. However, the low solubility values suggest that the activated carbons remain largely stable in aqueous environments, which is important for maintaining their performance in water treatment applications.

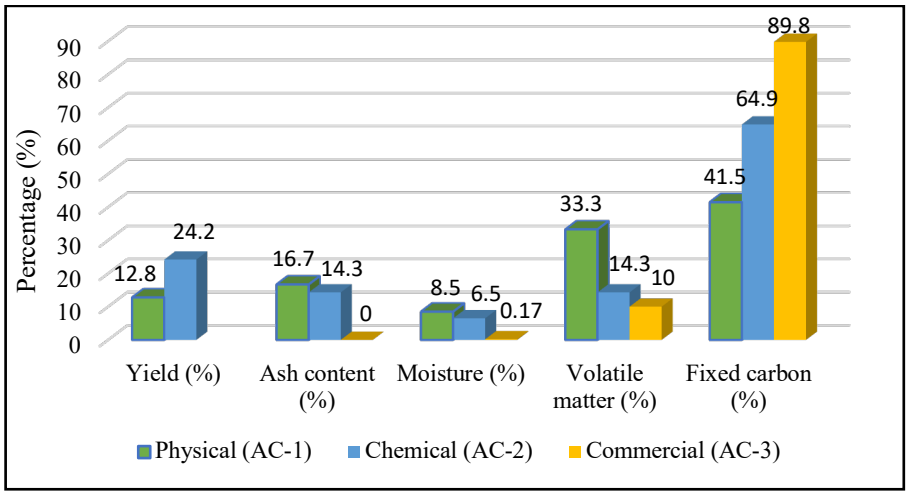

Figure 2: Yield and proximate analysis of AC-1, AC-2 and AC-3.

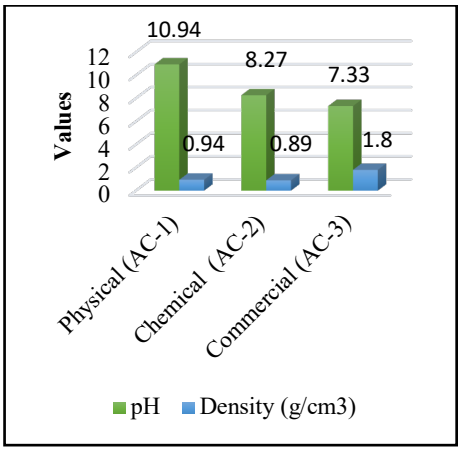

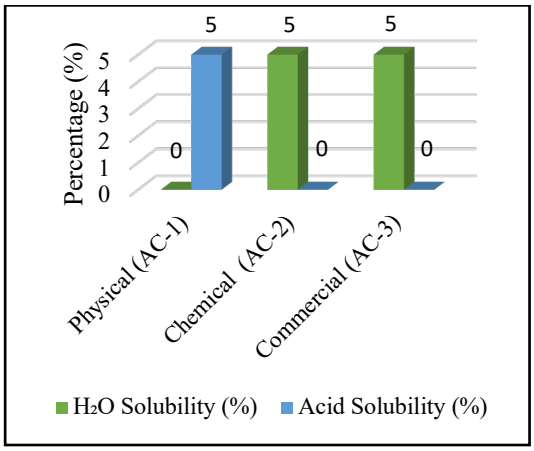

Figure 3: Density and pH of AC-1, AC-2 and AC-3. **Figure 4:** Water and acid solubility

4.2 Chemical Characteristics of Activated Carbon

4.2.1 Fourier Transform Infrared Spectroscopy Analysis

Figure 5 displays the FTIR spectrum of chemically activated carbon derived from waste paper (AC-2). The peaks observed provide insights into the functional groups present on the activated carbon surface. The peaks at 3679.7 cm^{-1} and 3712.2 cm^{-1} correspond to O-H stretching vibrations, likely indicating the presence of hydroxyl groups, which could be attributed to residual moisture or alcohol groups - a common feature in biomass-derived activated carbons [61,62].

Multiple peaks in the range of 2977.2 cm^{-1} to 2821.1 cm^{-1} indicate C-H stretching vibrations, suggesting some aliphatic character such as residual CH_2 and CH_3 groups originating from the organic components in the waste paper feedstock. The peak at 1055.3 cm^{-1} is likely due to P-O and P=O stretching in phosphate or phosphoric acid derivatives, a result of the phosphoric acid used during activation. This incorporation of phosphorus-containing groups is advantageous, as they can enhance the adsorption properties of the carbon [62].

The peaks at 1012.7 cm^{-1} and 1032.5 cm^{-1} are indicative of C-O stretching, typically associated with ether or alcohol groups, suggesting the presence of oxygen-containing functionalities that may enhance the carbon's hydrophilicity and interactions with polar molecules.

Overall, the FTIR spectrum reveals a combination of hydroxyl, aliphatic C-H, phosphorus-containing, and C-O groups. These functional groups contribute to the surface chemistry of the activated carbon, improving its adsorption capacity, particularly in aqueous applications. The phosphorus groups, derived from phosphoric

acid activation, are particularly beneficial for adding acidic sites, which further enhance adsorption potential of the adsorbent.

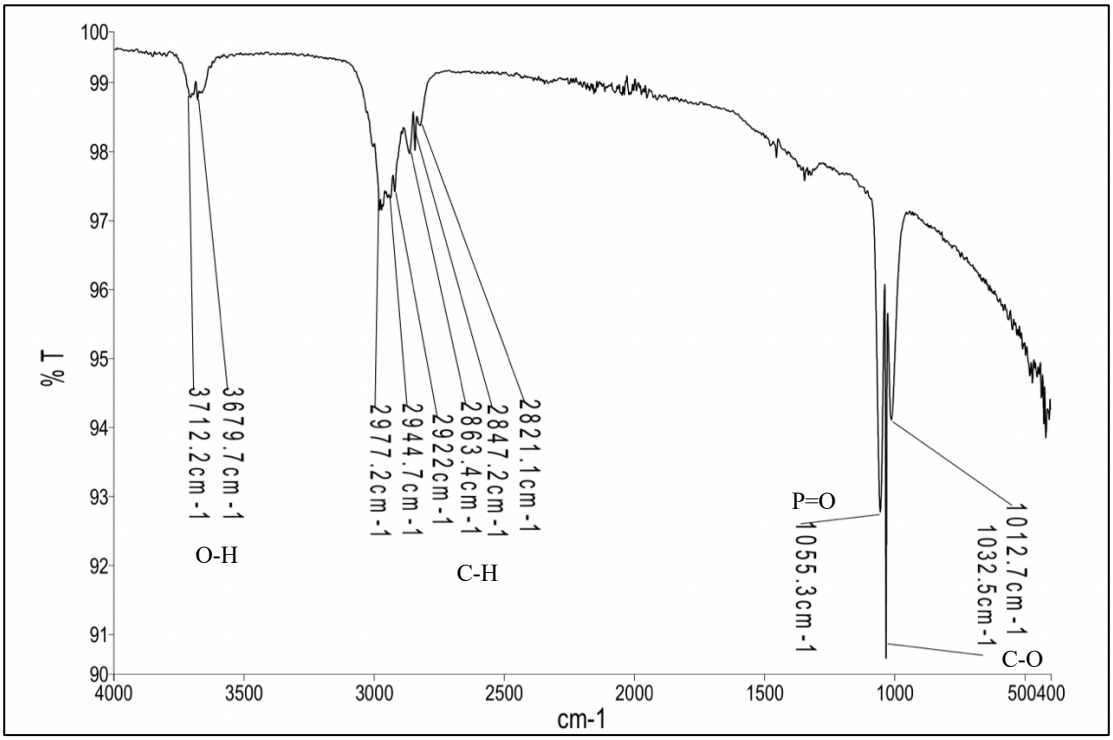

Figure 5: FTIR spectrum of activated carbon prepared from waste paper by chemical activation (AC-2)

Figure 6 presents the FTIR spectrum of physically activated carbon, highlighting two prominent peaks at 1416.3 cm^{-1} and 876.42 cm^{-1}. The peak observed at 1416.3 cm^{-1} is generally attributed to C=C stretching vibrations within aromatic rings, indicating aromatic structures within the carbon. This is a common feature in activated carbon, as carbonisation promotes the development of stable aromatic rings and conjugated double bonds, which enhance both structural stability and adsorption capabilities. This peak might also suggest minor C-O stretching from carboxylate ions (COO^{-}), hinting at the presence of residual oxygen-containing functional groups, which often remain even after physical activation processes [81].

In addition, the peak at 876.42 cm^{-1} is typically linked to C-H out-of-plane bending vibrations in aromatic rings, particularly those with isolated or substituted hydrogen atoms. In the context of activated carbons, this peak reflects the formation of polycyclic aromatic structures, indicating that the material has transitioned towards an aromatic, graphitic-like framework during activation. These structural transformations are particularly beneficial for adsorption, as the aromatic network allows for π-π interactions with organic pollutants, enhancing the material's ability to trap and retain various contaminants [81].

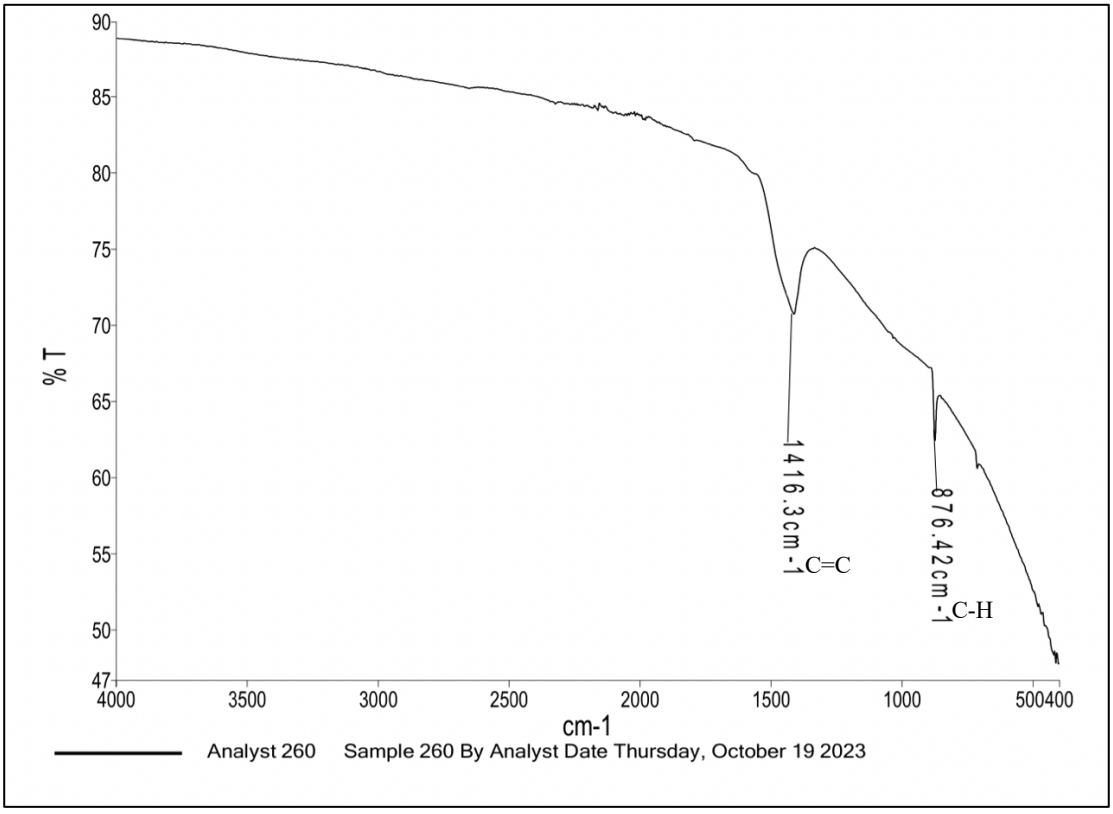

Figure 6: FTIR spectrum of activated carbon prepared from waste paper by physical activation (AC-1)

4.2.2 Scanning electron microscopy analysis

Scanning Electron Microscopy (SEM) provides valuable insights into the surface morphology of materials, revealing micrographs that display a variety of pores and

structures. Figures 7 and 8 showcase SEM images of activated carbon produced through two different activation methods: physical activation (figure 7) and chemical activation (figure 8).

The SEM images in Figure 7, representing physically activated carbon, exhibits a dense, bulk morphology with irregularly shaped granules and no visible microspheres. This is consistent with findings in physically activated carbon from other lignocellulosic sources, such as sawdust and starch, as noted in previous studies [82]. Physically activated carbons typically undergo high-temperature treatment in an inert or oxidising environment, leading to the removal of volatile components and pore formation. However, the structure produced often shows limited porosity and an uneven distribution of pores, with a less-developed network of accessible channels compared to chemically activated carbon. Additionally, areas with white residue are visible in Figure 7, which may indicate ash or residual minerals from the waste paper that were not entirely removed during activation.

In contrast, the SEM image in Figure 8, corresponding to chemically activated carbon, shows a much more porous structure and the presence of tubular carbon formations. This is largely due to the chemical activation process, where reagents like phosphoric acid interact with the precursor material to facilitate dehydration and expansion, promoting the formation of a more extensive pore network [62]. This method allows for a more uniform and developed porosity, resulting in enhanced accessibility and greater surface area.

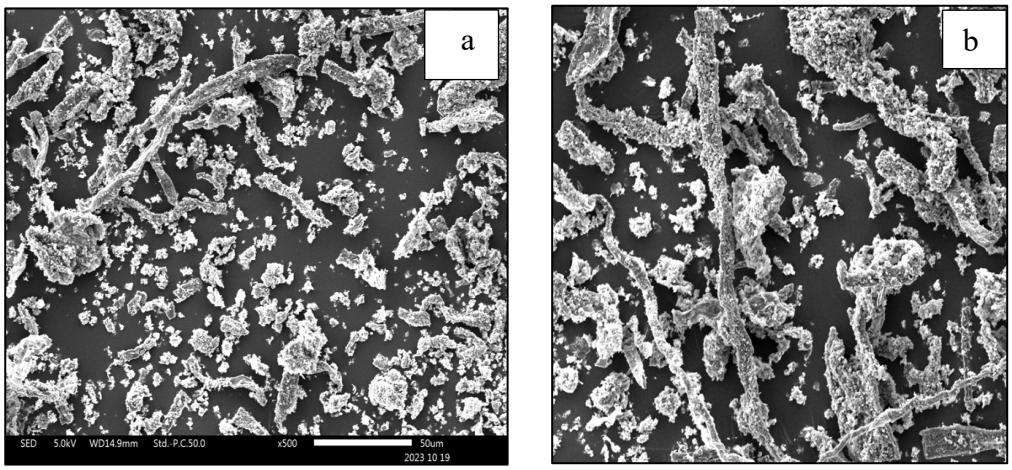

Figure 7: SEM images (a and b) of activated carbon prepared from waste copy paper through physical activation.

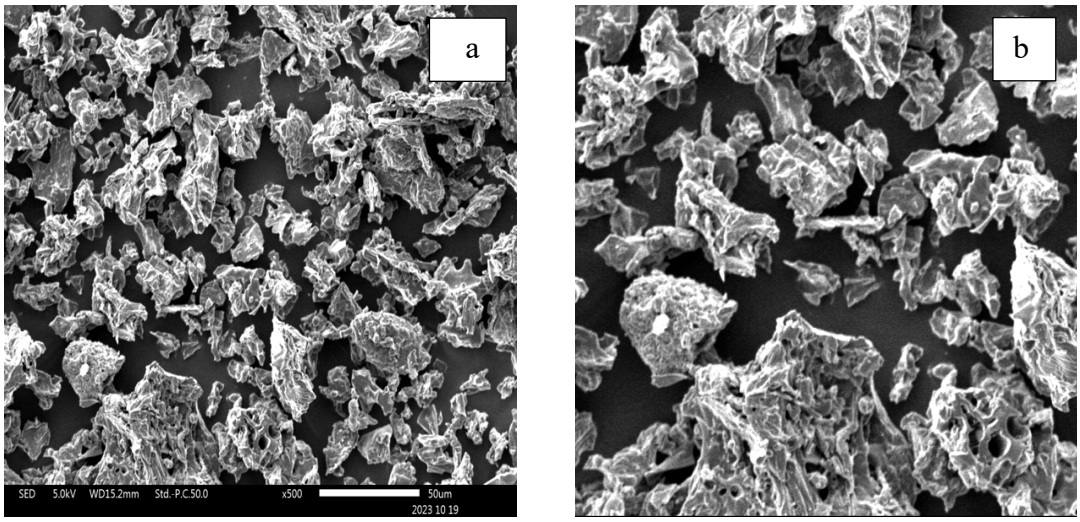

Figure 8: SEM images (a and b) of activated carbon prepared from waste copy paper by chemical activation.

4.2.3 X-Ray Diffraction Analysis

Figure 9 shows the XRD spectrum of AC obtained from waste paper through physical activation. The figure shows distinct peaks at 26.896°, 31.09°, 34.32° (highest intensity), 42.131°, 46.216°, 50.759°, 55.953°, 57.192°, 68.036°, and 77.121°. The peak around 26.896° corresponds to the (002) plane, which indicates the presence of graphitic carbon structures; this peak is typical in carbon materials and is associated

with stacked graphitic layers, *albeit* in a more disordered arrangement for activated carbons [83].

The peaks at 31.09°, 42.131°, and 50.759° may represent other graphitic planes such as (100) or (101) [83,84], often seen in disordered carbon and indicating polyaromatic layers within the structure. These planes contribute to the material's slightly crystalline nature due to regions of aligned carbon layers. Additionally, peaks in the 55-58° range (notably 55.953° and 57.192°) could suggest the presence of crystalline impurities or residual mineral content from the precursor or activation process.

Overall, the presence of multiple sharp peaks suggests a level of crystallinity higher than that of a fully amorphous carbon, likely due to partial graphitisation during physical activation. However, the carbon remains largely disordered, as indicated by the broadening and distribution of peaks. This combination of ordered (graphitic) and disordered regions typically enhances the activated carbon's surface area and porosity, making it suitable for adsorption applications.

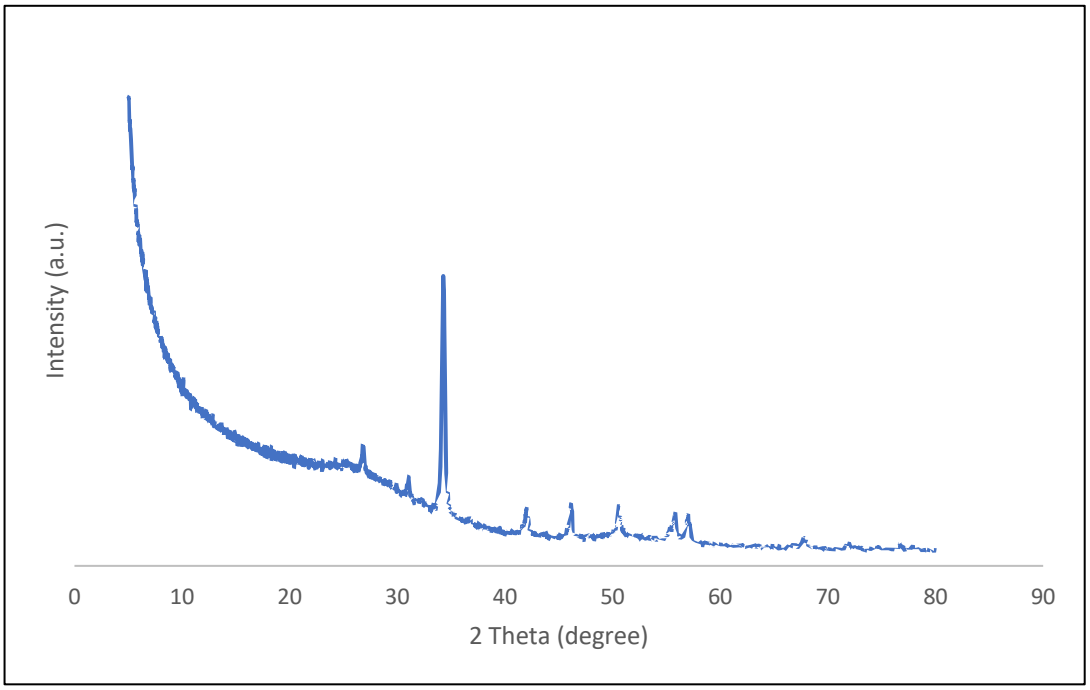

Figure 9: XRD Spectra of activated carbon prepared from waste paper by physical activation.

Figure 10 presents the XRD pattern of activated carbon prepared through phosphoric acid activation, where specific 2θ peaks reveal structural characteristics and possible phases within the carbon. The observed peaks at 23.397° and 25.744°, which fall within the typical range of 2θ ≈ 24-26°, are associated with the (002) plane of graphitic carbon [83]. These peaks suggest the presence of graphitic-like layers, however, the significant disorder indicated by the broadness of these peaks is characteristic of activated carbons.

This broad, less-defined region further supports the notion that the carbon structure lacks long-range order and is predominantly amorphous in nature.

Additionally, the peak at 50.759° could correspond to the (100) or (101) planes of disordered graphite, signifying areas of graphitic order, *albeit* minimal [83,84]. This peak may also indicate residual phosphorus-containing species embedded in the

carbon matrix due to phosphoric acid activation. Such phosphorus residues can contribute to unique structural features and may impact the material's surface chemistry and adsorption properties, potentially enhancing the activated carbon's effectiveness in specific applications. Overall, the XRD pattern reflects a largely disordered carbon structure with small graphitic domains, consistent with the expected properties of chemically activated carbon.

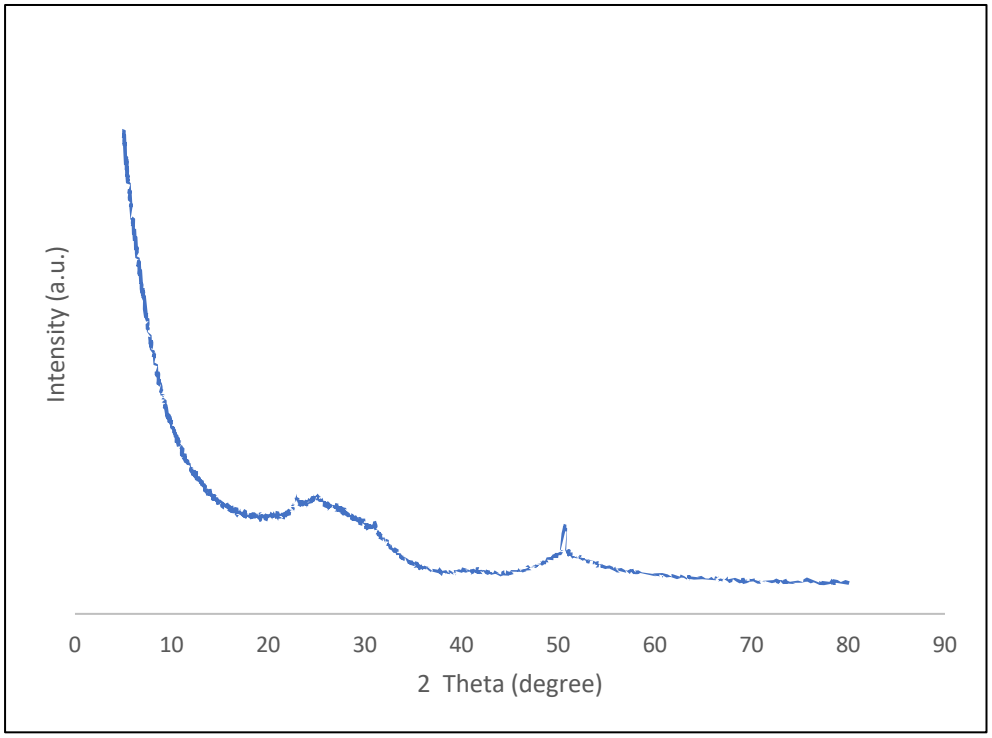

Figure 10: XRD Spectra of activated carbon from waste paper prepared by chemical activation.

In summary, the XRD patterns of AC- 1 (figure 9) and AC-2 (figure 10) show clear differences which could be linked to their different activation methods, AC-1 had more and sharper peaks, meaning it has some ordered, graphitic structures [83]. In contrast, AC-2 showed broader peaks, indicating that its structure is mostly disordered or amorphous [83, 84].

4.2.4 Brunauer-Emmett-Teller Analysis

Table 2 provides the BET analysis results for two activated carbon samples, AC-1 and AC-2, which were prepared through physical and chemical activation, respectively. The data reveal key differences between the two. AC-2 shows a notably higher specific surface area of 678.01 m^2/g compared to 455.22 m^2/g for AC-1, reflecting the enhanced porosity typical of chemical activation. Additionally, the t-Plot external surface area for AC-2 is 262.15 m^2/g, higher than that of AC-1 (175.08 m^2/g), indicating a greater contribution from meso- and macropores in AC-2. The Barrett-Joyner-Halenda (BJH) method estimates pore surface area specifically for mesopores and larger pores. The BJH adsorption and desorption cumulative surface areas also favour AC-2 (255.84 m^2/g and 237.66 m^2/g) over AC-1 (207.38 m^2/g and 237.95 m^2/g), further highlighting enhanced mesoporosity for AC-2, which can be advantageous for adsorbing larger molecules.

The t-plot micropore volume for AC-2 is 0.21573 cm^3/g, surpassing that of AC-1 (0.14577 cm^3/g), suggesting that AC-2 has a greater capacity for adsorbing smaller molecules due to its higher microporosity. Interestingly, the average pore diameter for AC-2 is much larger (294.28 Å) than that of AC-1 (112.93 Å), implying a broader range of pore sizes, which can facilitate adsorption of larger molecules or be beneficial for liquid-phase adsorption.

Overall, AC-2, with its increased surface area, higher pore volume, and larger average pore diameter, appears to be more versatile, suitable for a wider range of adsorption applications, from small molecules to larger organic contaminants. These characteristics align with the expected impact of chemical activation, which promotes

both microporosity and mesoporosity, making AC-2 more adaptable compared to the physically activated AC-1.

Table 2: Results obtained from the BET analysis of activated carbon

Activated Carbon	Specific Surface Area (m^2/g)	t-plot External Surface Area (m^2/g)	BJH Adsorption Cumulative Surface Area (m^2/g)	BJH desorption Cumulative Surface Area (m^2/g)	t-Plot micropore volume (cm^3/g)	Adsorption average pore diameter (Å)
Physical activation	455. 22	175.08	207.38	237.95	0.14577	112.93
Chemical activation	678.01	262.15	255.84	237.66	0.21573	294.28

4.2.5 Langmuir and Freundlich adsorption isotherm Analysis

To evaluate the adsorption characteristics of the prepared activated carbon samples, the Langmuir and Freundlich adsorption isotherm models were employed using nitrogen gas as the adsorbate. These models were applied separately to physically activated carbon (AC-1) and chemically activated carbon treated with phosphoric acid (AC-2) and the results were compared to understand the influence of activation method on adsorption behaviour.

The adsorption behavior of nitrogen gas on the physically activated carbon (AC-1) was evaluated using both the Freundlich and Langmuir isotherm models. The Freundlich adsorption isotherm plot (figure 11) demonstrated a moderate correlation (R^2 = 0.7486), suggesting partial adherence to the model's assumption of heterogeneous surface adsorption. From the slope (0.1535) and y-intercept (1.8806) of the linearized

plot, the Freundlich constant (n = $\frac{1}{slope}$) was calculated as 6.51, and the adsorption capacity ($K_f = 10^{y-intercept}$) as 75.96 cm^3/g. An n-value greater than 1 signifies favorable adsorption [89], and the relatively high K_f reflects a notable adsorption capacity of nitrogen, *albeit* with limited surface heterogeneity.

Conversely, the Langmuir isotherm plot (figure 12) displayed a highly linear relationship ($R^2 = 0.9985$), indicating that the adsorption process aligns closely with the Langmuir model's assumptions of monolayer coverage on a uniform surface [90]. The slope (0.0055) and y-intercept (0.0786) were used to determine the maximum adsorption capacity ($Q_m = \frac{1}{slope}$ = 181.81 cm^3/g) and the Langmuir constant (b = $\frac{1}{(y-intercept)(Qm)}$ = 0.0700 1/mmHg). The high Q_m value (181.81 cm^3/g) indicates that the physically activated carbon has a large surface area and high capacity for nitrogen gas adsorption [62, 90]. The moderate b value (0.0700 $mmHg^{-1}$) suggests favorable but weak interactions, typical of physisorption [19]. Therefore, the Langmuir model best describes the adsorption behaviour of nitrogen on physically activated carbon (AC-1), highlighting its monolayer adsorption capacity and surface uniformity [73].

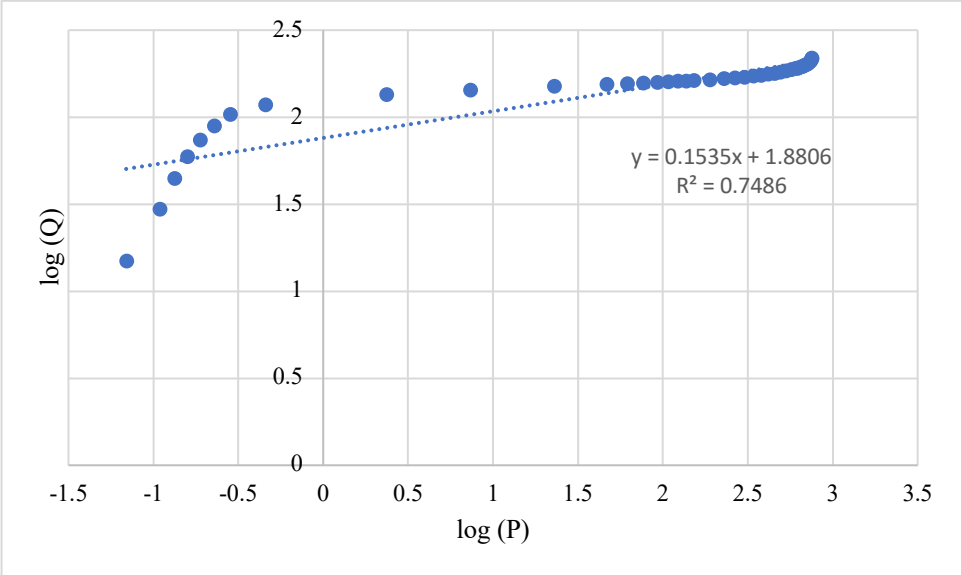

Figure 11: Freundlich linear plot obtained for the activated carbon prepared using physical activation.

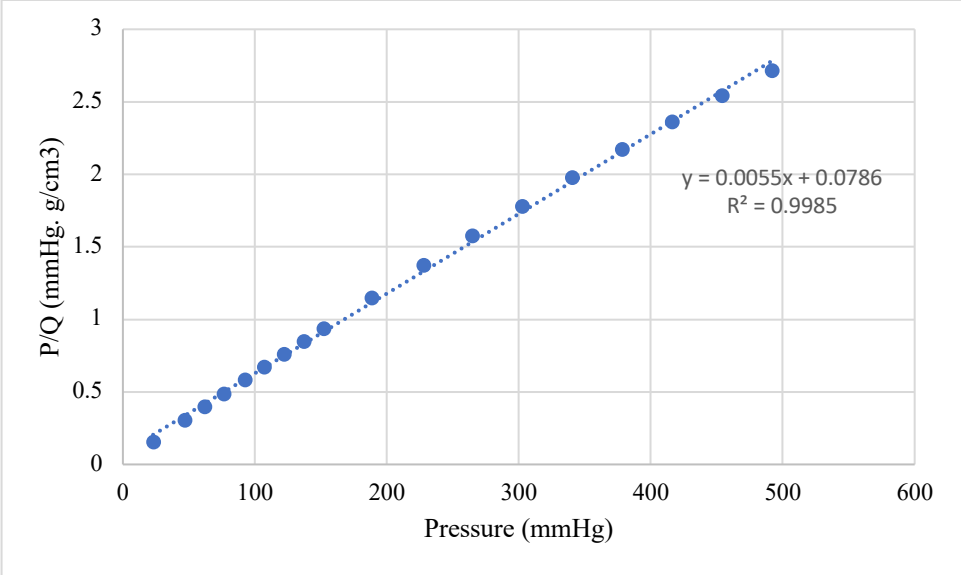

Figure 12: Langmuir linear plot obtained for the activated carbon prepared through physical activation.

Figure 13 the adsorption results for chemically activated carbon (AC-2) showed that the Langmuir model had a stronger fit (R^2 = 0.9961) compared to figure 14 for the

Freundlich model (R^2 = 0.8106), indicating that nitrogen gas adsorption occurred mainly as a monolayer on a uniform surface**.** The high Q_m value (263.16 cm^3/g) suggests a large adsorption capacity, which reflects the well-developed porous structure created by phosphoric acid activation [11, 62]. The b value (0.03831 1/mmHg) also indicates favorable but physical adsorption. Although the Freundlich model also showed favorable adsorption with n = 5.75 and K_f = 93.26 cm^3/g**,** the lower R^2 suggests it fits the data less accurately than the Langmuir model. Overall, the Langmuir model better describes the adsorption behavior of this chemically activated carbon.

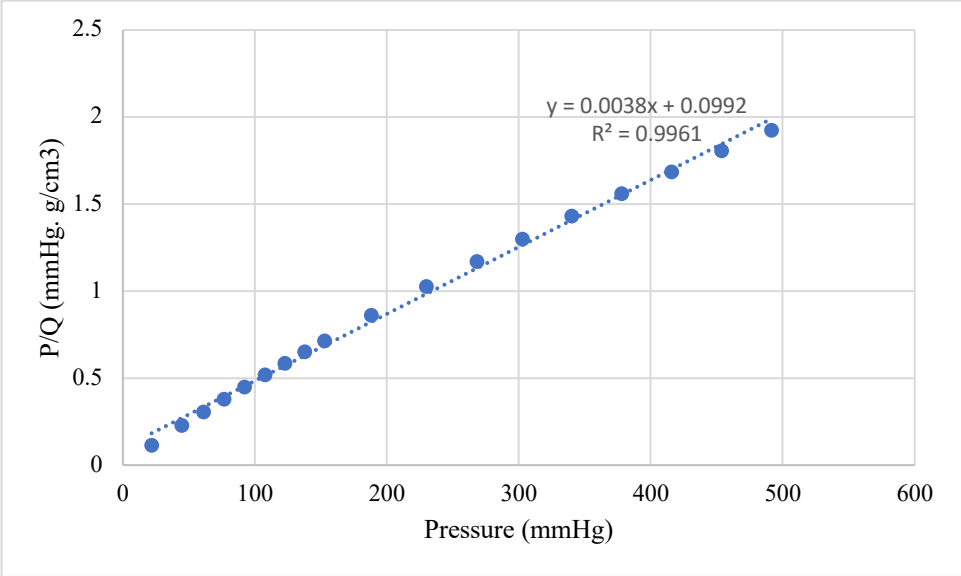

Figure 13: Langmuir linear plot obtained for the activated carbon prepared by chemical activation using phosphoric acid.

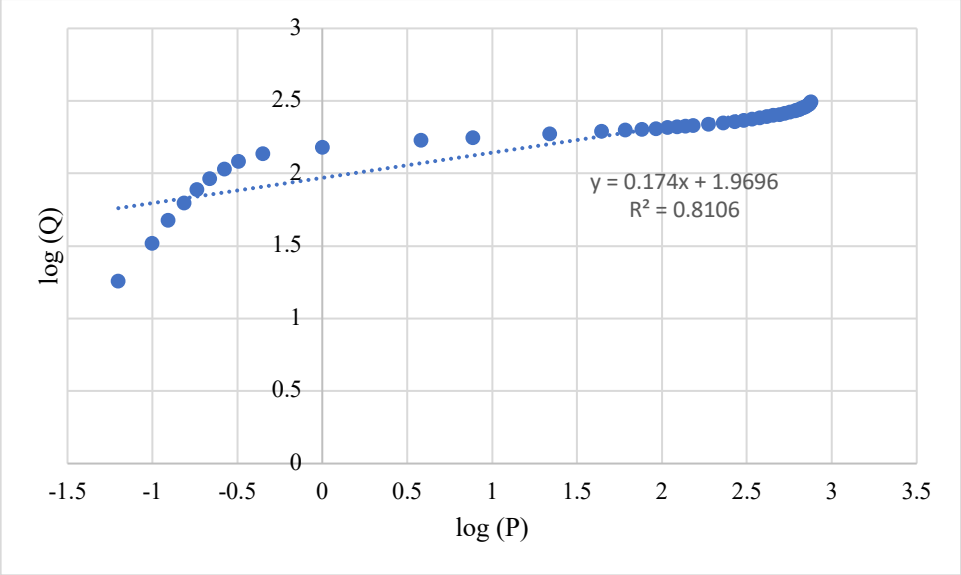

Figure 14: Freundlich linear plot for prepared activated carbon Chemical activation using phosphoric acid.

Both physically (AC-1) and chemically (AC-2) activated carbon samples demonstrated favorable adsorption characteristics, but the chemically activated carbon exhibited superior performance overall. The Langmuir model provided a better fit for both ACs, suggesting that adsorption occurs primarily as a monolayer on uniform surfaces. AC-2, which was activated using phosphoric acid, had a higher monolayer adsorption capacity (Q_m = 263.16 cm^3/g**)** than AC-1 (Q_m = 181.81 cm^3/g**),** indicating a greater surface area and more efficient pore structure. While both isotherms showed favorable adsorption intensity (n > 1), the stronger correlation (R^2 = 0.9961) and higher Q_m of AC-2 suggest it is more effective. Therefore, chemically activated carbon is more suitable for water treatment, especially in removing contaminants such as dyes and heavy metals, due to its enhanced adsorption efficiency and surface characteristics.

4.3 Wastewater treatment with Activated Carbon

The efficiency of water treatment using the prepared activated carbons- physically activated (AC-1), chemically activated with phosphoric acid (AC-2), and commercially available activated carbon (AC-3) - was assessed by analysing influent (raw) and effluent (semi-treated) water samples before and after treatment. The removal efficiency (RE) was used as a key performance indicator. Table 3 presents the physicochemical characteristics of the untreated wastewater collected from the Gammams treatment facility.

To evaluate the performance of the activated carbons in enhancing water quality, both raw (influent) and semi-purified (effluent) domestic wastewater samples were treated. The initial quality parameters of the raw water included a total dissolved solids (TDS) concentration of 785 mg/L, dissolved oxygen (DO) of 0.55 mg/L, electrical conductivity of 2384 µS/cm, turbidity of 355 NTU, and salinity of 0.57 PSU- values typical of untreated domestic effluent. The influence of activated carbon dosage, contact time, and temperature on the removal of these contaminants was investigated.

Table 3: Water quality parameters of Gammams Raw water.

Physico-chemical parameters	**Influent**	**Effluent**
TDS (mg/L)	785	698
DO (mg/L)	0.55	5.80
Conductivity (µS/cm)	2384	1594
Turbidity (NTU)	355	2.31
Salinity (PSU)	0.57	0.41

4.3.1 Effect of dosage on the removal efficiency of contaminants

The effect of AC dosage on water treatment was studied at room temperature with the contact time of 60 minutes. 0.05, 0.1 and 0.2 g of AC were added to 100 ml of wastewater. Data in figures 15 through 19 illustrate the removal efficiencies for pollutants at various AC dosages. Turbidity demonstrated the highest removal efficiency across all three ACs (AC-1, AC-2, and AC-3), consistently achieving over 90% removal. Notably, AC-2 achieved the highest turbidity reduction, with a 97.2% removal efficiency at a 0.05 g dosage. Dissolved oxygen (DO) showed the next highest removal rates, with AC-1 achieving an 89.3% reduction at a 0.2 g dosage. Conductivity removal ranked third, with the most effective reduction being 57.34%, observed with AC-1 at a 0.1 g dosage. In contrast, total dissolved solids (TDS) and salinity exhibited lower removal efficiencies, with TDS reaching a maximum of 15.8% at a 0.2 g dosage in AC-1.

The results show that AC-1 (physically activated carbon) achieved the highest removal efficiency for most water quality parameters. However, all three activated carbons (AC-1, AC-2, and commercial AC-3) demonstrated effective contaminant removal from domestic wastewater, with the prepared carbons (AC-1 and AC-2) performing comparably to the commercial product.

To add on, figures 15 to 19 also present the removal efficiencies for various parameters in the semi-purified wastewater (effluent). Among the effluent parameters, conductivity exhibited the highest removal efficiency, reaching 53.7% with a 0.1 g dosage of AC-1. This was followed by turbidity, which was reduced by 49.78% with AC-3 at the same dosage, and TDS, which showed a removal efficiency of 35.36% with a 0.2 g dosage of AC-3. Salinity followed with a 24.39% removal efficiency at a

0.1 g dosage of AC-1, and DO displayed the lowest removal efficiency, with a reduction of 6.9% observed in both AC-1 and AC-3.

A comparison between the removal efficiencies in the influent (raw water) and the effluent shows lower removal rates in the effluent, as detailed in figures 15 to 19 as well as tables 11– 16 for each parameter. This difference can be attributed to the higher initial concentration of contaminants in the raw water, which provides more adsorption sites for the AC, resulting in a more efficient adsorption process [19].

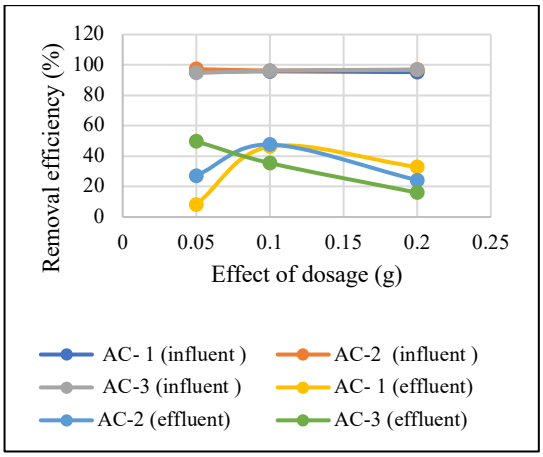

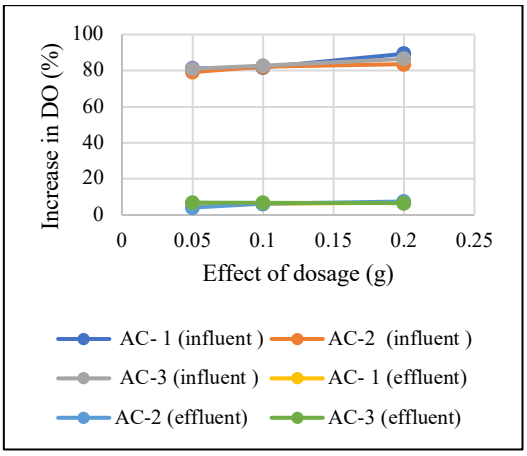

Figure 15: Effect of adsorbent dosage on turbidity removal efficiency. **Figure 16:** Effect of adsorbent dosage on the removal efficiency of dissolved oxygen (DO).

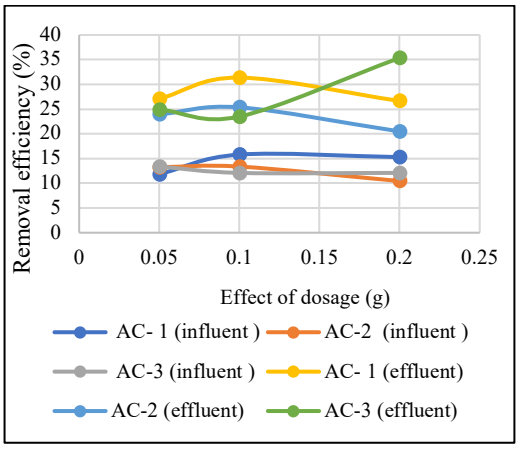

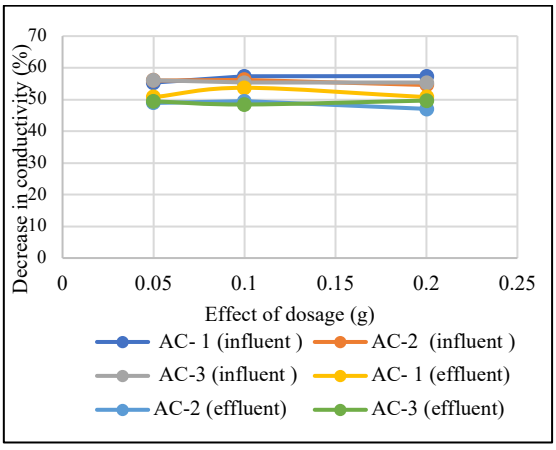

Figure 17: Effect of adsorbent dosage on TDS removal efficiency. **Figure 18:** Effect of adsorbent dosage on conductivity removal efficiency

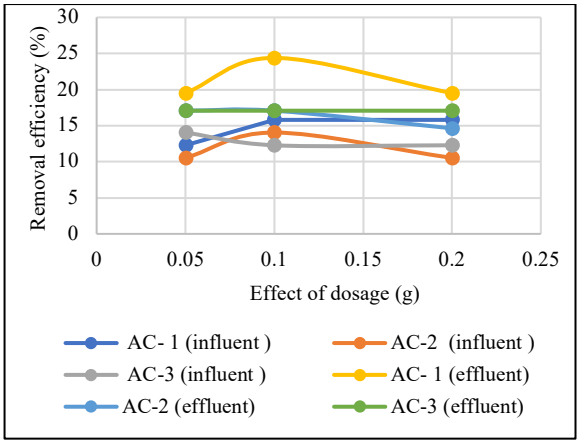

Figure 19: Effect of adsorbent dosage on the salinity removal efficiency.

4.3.2 Effect of contact time on the removal efficiency of contaminants

The impact of contact time on wastewater treatment was examined by adding 0.2 g of each activated carbon to 100 ml of wastewater (both influent and effluent) at room temperature, with treatment durations ranging from 10 to 120 minutes.

Figures 20 to 24 and tables 17 to 22 (appendix) detail the impact of contact time on the removal efficiencies of contaminants in both influent and effluent domestic wastewater treated with the prepared activated carbons (AC-1 and AC-2) and commercial activated carbon (AC-3).

In the influent samples, dissolved oxygen (DO) and turbidity show the highest removal efficiencies, exceeding 80% across all ACs. Notably, AC-1 demonstrates the greatest efficiency in reducing turbidity, reaching 97.66% at 60 minutes. The observed trend of increased turbidity removal with extended contact time suggests that prolonged exposure allows for more thorough interaction between the AC particles and suspended solids [85,86]. This extended exposure likely promotes enhanced adsorption, as contaminants have more time to encounter and bind to the AC surface [86]. DO also shows a high removal rate, with AC-1 achieving 90.76% efficiency, followed by conductivity with a peak removal of 60.99% using AC-1. In contrast, TDS

and salinity removal are less efficient, staying below 40%, likely due to their relatively lower adsorptive affinity on the AC's surface or competition for adsorption sites from more strongly binding contaminants.

For the effluent samples, similar trends are observed, though the removal efficiencies are generally lower compared to the influent. This may be due to the reduced concentration of contaminants in the effluent, as it has already undergone partial treatment, which lowers the likelihood of effective adsorption by AC. In the effluent, AC-3 achieves a notable removal efficiency of 61.47% for turbidity within 10 minutes. The negative removal efficiency observed for turbidity at early contact times for AC-2 suggests an increase in turbidity levels post-treatment. This is likely due to the release of fine activated carbon particles into the solution or incomplete adsorption during the initial stages of treatment [85]. Conductivity removal in the effluent shows a moderate efficiency range of 48.18% to 50.56% across all ACs. Meanwhile, DO, TDS, and salinity exhibit relatively low removal rates, consistent with the lower contaminant levels in the effluent compared to influent, limiting the ACs' overall adsorption performance for these parameters.

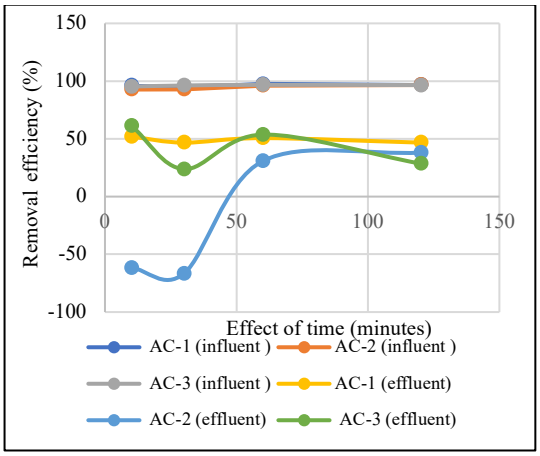

Figure 20: Effect of contact time on turbidity removal efficiency.

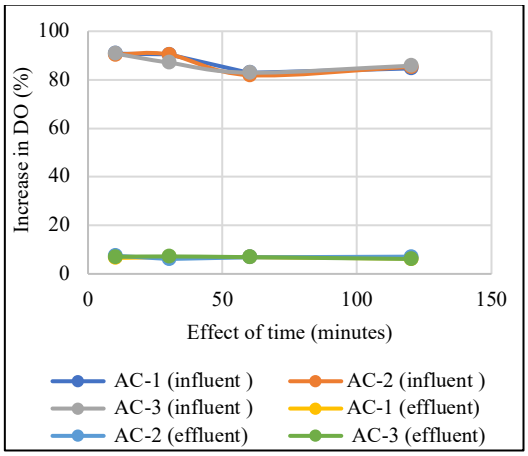

Figure 21: Effect of contact time on DO removal efficiency.

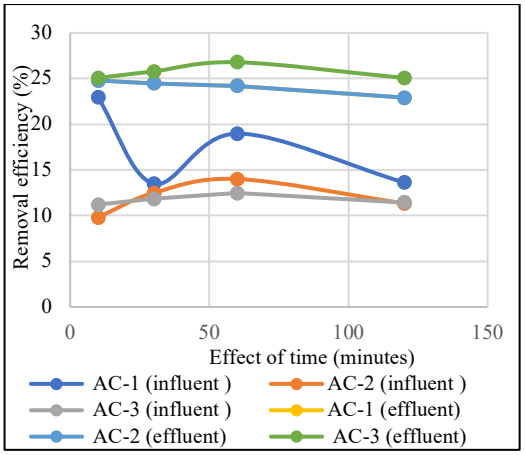

Figure 22: Effect of contact time on TDS removal efficiency.

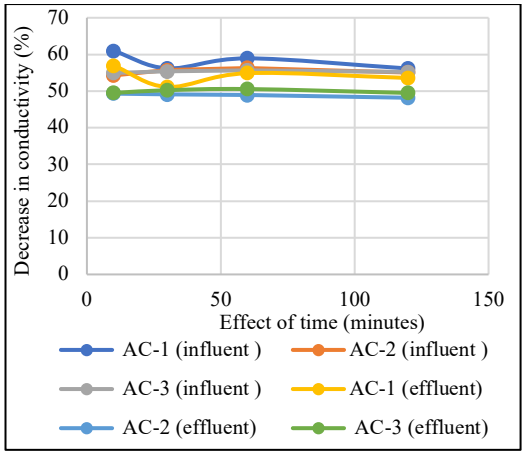

Figure 23: Effect of contact time on conductivity removal efficiency.

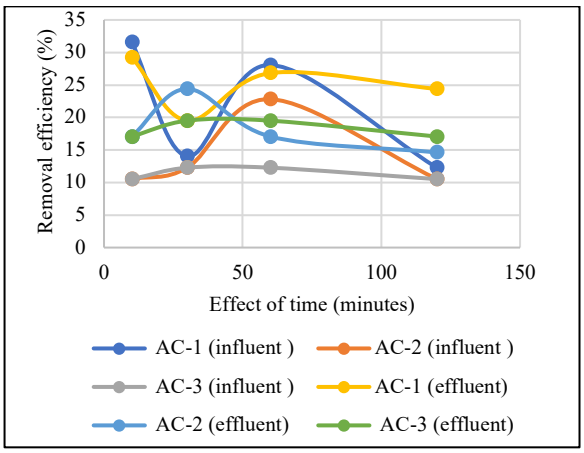

Figure 24: Effect of contact time on salinity removal efficiency.

4.3.3 Effect of Temperature on the removal efficiency of contaminants

Figures 25 – 29 and tables 23 – 25 (in appendix) present the impact of temperature on the removal efficiency of various contaminants in influent wastewater treated with activated carbons. The data reveals a direct relationship between temperature and removal efficiency: higher temperatures consistently improve the removal of contaminants. This increase in efficiency with temperature is likely due to enhanced molecular activity, which may facilitate better interaction between the activated carbon and the contaminants, thus improving adsorption [85, 86].

As illustrated in Figure 41 (appendix), the visual changes in influent samples treated with AC-2 at different temperatures (from 28.0 to 90.0 °C) confirm that the removal of contaminants intensifies with rising temperatures. In the influent samples, turbidity removal remains consistently high across all ACs, exceeding 93%, with a peak removal efficiency of 96.28% at 90 °C. DO removal efficiency also surpasses 86% for all ACs, reaching a maximum of 92% at 90 °C. Conductivity shows significant removal efficiency above 50% across all ACs, peaking at 64.01% at 90 °C. However, TDS and salinity removal efficiencies remain comparatively low, both staying below 40%, even at elevated temperatures. The lower removal efficiency for TDS and salinity could be attributed to the stable and dissolved nature of these ions, which may not readily bind to the AC surface.

In contrast, tables 26 to 28 and figures 25 to 29 detail the effects of temperature on contaminant removal in the effluent samples. Here, even as temperatures increase, the removal efficiency remains relatively low across most parameters. As shown in fugure 28 the highest removal efficiency observed in the effluent is for conductivity, which achieves 54.83% with AC-1. Turbidity (figure 25), however, shows an unusual trend where its values increase rather than decrease, suggesting possible desorption or inadequate adsorption of suspended solids in partially treated effluent [85].

The overall lower removal efficiency in the effluent compared to the influent at high temperatures could be due to the reduced levels of contaminants in the semi-treated effluent, which minimizes the availability of adsorbable particles. Furthermore, high-temperature conditions might cause desorption or disrupt the binding of certain contaminants that were previously adsorbed in the partially treated water, impacting parameters like turbidity in particular.

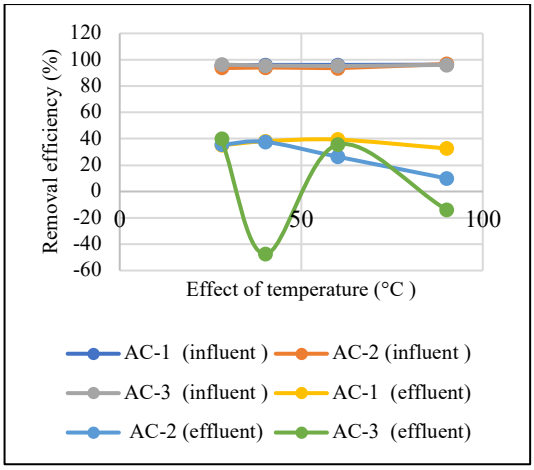

Figure 25: Effect of temperature on turbidity removal efficiency.

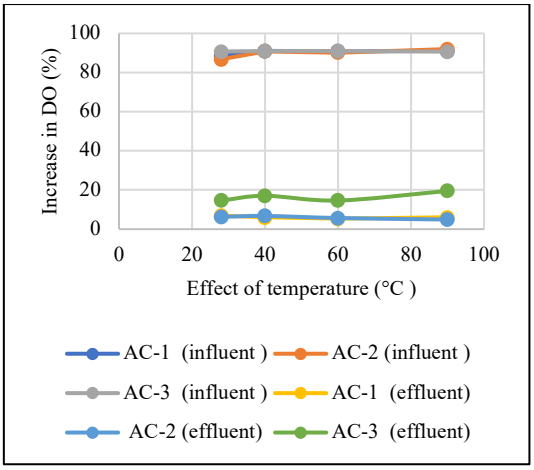

Figure 26: Effect of temperature on the removal efficiency of DO.

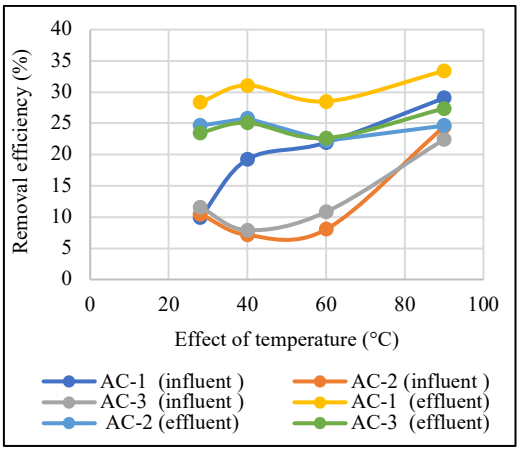

Figure 27: Effect of temperature on TDS removal efficiency.

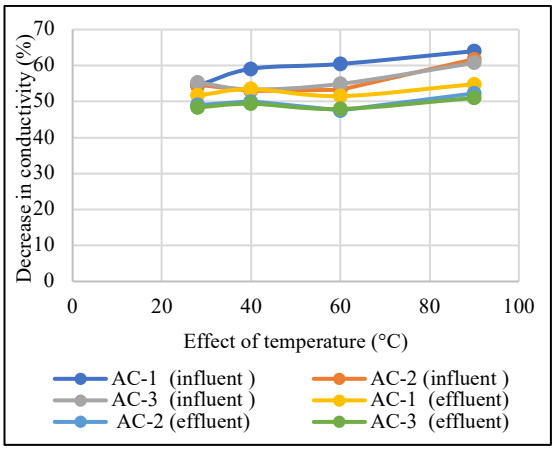

Figure 28: Effect of temperature on conductivity removal efficiency.

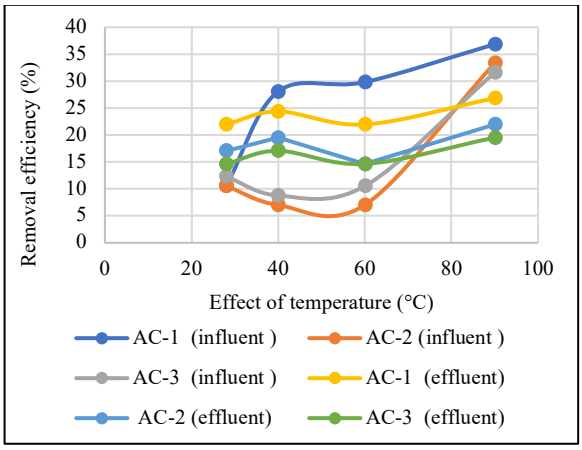

Figure 29: Effect of temperature on the salinity removal efficiency.

4.4 Results of dyes (MB and MO) and Cu^{2+} from $CuSO_4$

In this study, only AC-2 the activated carbon derived from waste paper using phosphoric acid as the activating agent was tested to assess its efficiency in removing methylene blue, methyl orange, and Cu^{2+}. The investigation further explored how variables such as contact time, temperature, pH, and concentration affected the removal efficiency.

4.4.1 Effect of Time on the removal efficiency of contaminants

0.05 g of ACs were used to treat 25 ml of Cu^{2+}, MB and MO with concentrations of 100 mg/L at room temperature (28.0°C). The time ranges from 10 to 120 minutes.

Table 4 and figure 30 present the impact of contact time on the removal efficiency of Cu^{2+}, MB, and MO when treated with AC-2 . Table 4 specifically displays the absorbance values of the solutions before and after treatment with AC. It is evident from the table that absorbance values decreased significantly following AC treatment, indicating successful adsorption and removal of contaminants. This reduction in absorbance reflects the AC's effectiveness in decreasing the concentration of these substances in the solutions.

The graph in Figure 30 further illustrates this trend, showing that MO exhibits the highest removal efficiency, consistently close to 100% regardless of the duration of treatment. This result suggests that the AC has a strong affinity for MO molecules, allowing for rapid and effective adsorption even at shorter contact times [61,90].

For MB, the removal efficiency starts around 80% within the first 10 and 30 minutes of treatment. As contact time extends, the removal efficiency for MB gradually improves, reaching nearly 100% at 60 and 120 minutes. This pattern indicates that

prolonged exposure allows for more MB molecules to be adsorbed by the available active sites on the AC surface [32].

In the case of Cu^{2+}, removal efficiency also increases with extended contact time, but the values remain below 40% across all time intervals.

Table 4: Effect of Time for removal MO, MB and Cu^{2+} in 100 mg/L concentration.

Time (mins)	**Absorbance before treatment (A)**			**Absorbance after treatment (A)**		
	MO	**MB**	**Cu^{2+}**	**MO**	**MB**	**Cu^{2+}**
10	3.8995	3.2412	0.0989	0.8777	0.1105	0.0867
30	3.8995	3.2412	0.0989	0.8897	0.0639	0.0731
60	3.8995	3.2412	0.0989	0.1863	0.0559	0.0706
120	3.8995	3.2412	0.0989	0.1897	0.0567	0.0631

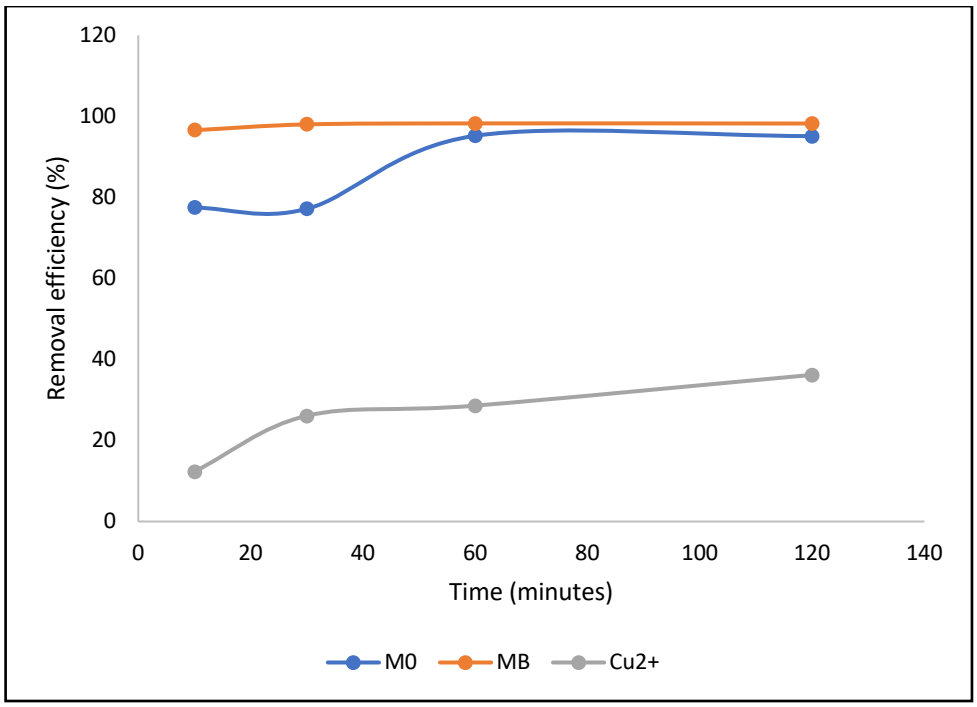

Figure 30: Effect of time on the removal efficiency of MO, MB and Cu^{2+}

4.4.2 Effect of Temperature

0.05 g of ACs were used to treat 25 ml of Cu^{2+}, MB and MO with concentrations of 100 mg/L at different temperatures, ranging from 28.0 to 80 °C. This was done for 60 minutes.

Table 5 and figure 31 illustrate the effect of temperature on the removal efficiency of MB, MO and Cu^{2+} when treated with activated carbon. As temperature increases, an overall improvement in removal efficiency is observed for all contaminants. MB exhibits the highest removal efficiency, reaching 98.70% at 80°C, suggesting that higher temperatures enhance the adsorption capacity of the activated carbon for MB. Similarly, MO shows a high removal efficiency of 94.19% at 80°C, indicating that temperature positively influences its adsorption as well, though slightly less than MB.

In contrast, although the removal efficiency of Cu^{2+} also increases with temperature, the values remain relatively low, with a maximum efficiency of only 21.74% at 80°C.

Table 5: Effect of Temperature for removal MO, MB and Cu $^{2+}$ in 100 mg/L concentration.

Temperature (°C)	**Absorbance before treatment (A)**			**Absorbance after treatment (A)**		
	MO	**MB**	**Cu^{2+}**	**MO**	**MB**	**Cu^{2+}**
Room temperature, 28.0	3.8995	3.2412	0.0989	0.7860	0.0669	0.0887
40.0	3.8995	3.2412	0.0989	0.4919	0.0530	0.0818
60.0	3.8995	3.2412	0.0989	0.4615	0.0537	0.0802
80.0	3.8995	3.2412	0.0989	0.2266	0.0506	0.0774

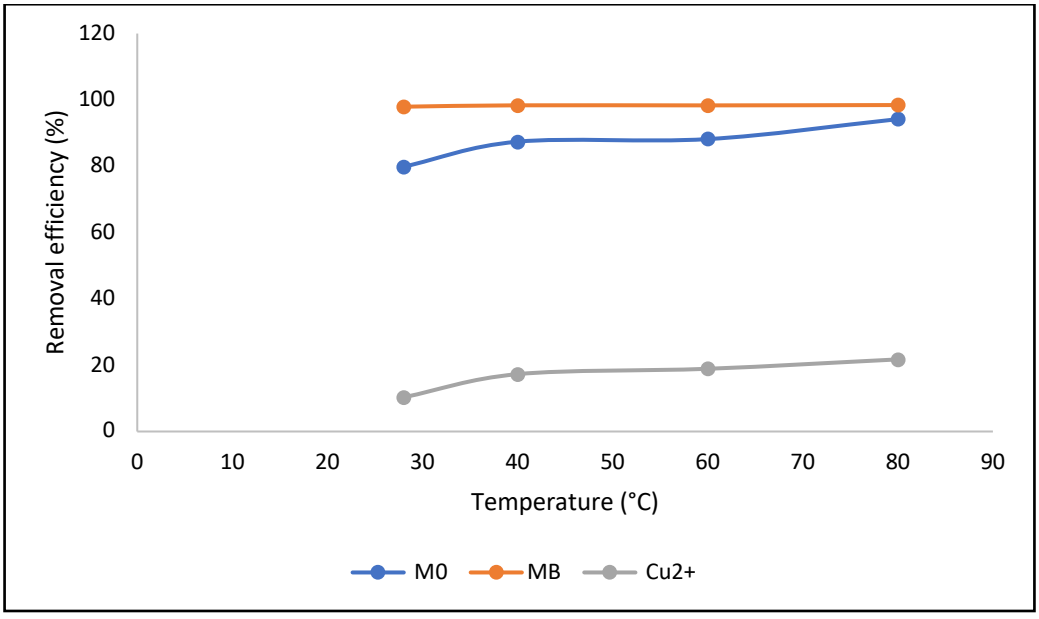

Figure 31: Effect of temperature on the removal efficiency of MO, MB and Cu^{2+}

4.4.3 Effect of pH

Table 6 presents absorbance values for the untreated and treated solutions (MO, MB and Cu^{2+}) after the application of activated carbon (AC-2). Additionally, Figure 32 highlights that as pH increases, the removal efficiency declines. For methylene blue, the maximum removal efficiency is observed at a low pH of 2, achieving 97.71%. This suggests that acidic conditions favour the adsorption of MB, likely due to the increased positive surface charge on the AC, which enhances interactions with the dye molecules [11, 61]. In contrast, the removal efficiency of Cu^{2+} remains consistently low, below 40%, regardless of pH variation. The highest efficiency for Cu^{2+} is 39.94%, occurring at a pH of 4, indicating limited effectiveness of AC for this metal ion across pH levels.

Table 6: Effect of pH for removal MO, MB and Cu^{2+} in 100 mg/L concentration.

pH	**Absorbance before treatment (A)**			**Absorbance after treatment (A)**		
	MO	**MB**	**Cu^{2+}**	**MO**	**MB**	**Cu^{2+}**
2	3.8995	3.2412	0.0989	0.1398	0.0743	0.0599
4	3.8995	3.2412	0.0989	0.1367	0.0818	0.0594
8	3.8995	3.2412	0.0989	0.1300	0.0811	0.0622
12	3.8995	3.2412	0.0989	0.3788	0.0948	0.0622

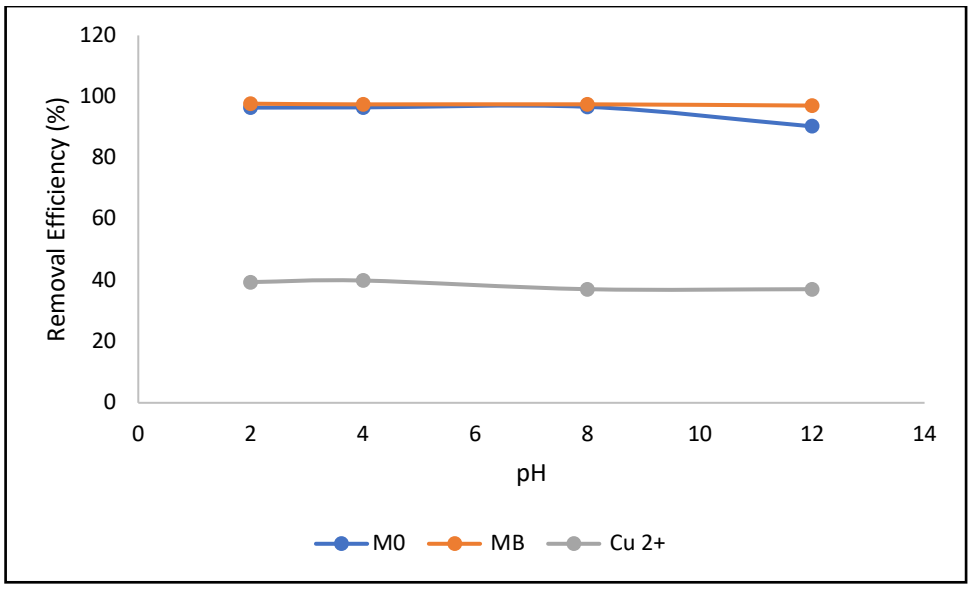

Figure 32: Effect of pH on the removal efficiency of MO, MB and Cu^{2+}

4.4.4 Effect of Concentration

The graph in figure 33 shows the removal efficiency of MO, MB, and Cu^{2+} when treated with activated carbon (AC- 2) produced from waste paper, chemically activated with phosphoric acid, across different concentrations (25, 50, 100, and 150 mg/L).

Methyl Orange: The removal efficiency for MO remains consistently high across the concentration range, close to 100%. This suggests that the AC from waste paper has a high affinity for MO, likely due to the AC's porous structure and surface characteristics, which facilitate strong interactions with the dye molecules. The consistently high removal indicates that even at higher concentrations, the AC capacity is not easily saturated with MO, allowing for effective adsorption. Figure 43 illustrates the removal of MO at various concentrations, showcasing a transition from an orange solution to a clear one.

Methylene Blue: The removal efficiency of MB starts high, close to 100% at lower concentrations (25 mg/L), but shows a noticeable decline as the concentration increases. By around 100 mg/L, the removal efficiency drops significantly, indicating

that as MB concentration increases, the AC begins to reach its saturation point, where it can no longer effectively adsorb additional dye molecules. This decline suggests that the adsorption sites for MB become saturated faster than for MO, possibly due to the size or interaction type of MB molecules with the AC surface. Figure 44 shows the removal of MB from different concentration showing from blue to clear solution.

Cu^{2+}: The removal efficiency of Cu^{2+} is substantially lower compared to MO and MB across all concentrations, starting around 60% and declining further as the concentration increases. Phosphoric acid activation primarily develops microporous structures ideal for organic molecules, making it less efficient in adsorbing ionic compounds like Cu^{2+} [90].

Overall, the graph shows that chemically activated carbon derived from waste paper is effective in removing dyes; particularly MO-even at higher concentrations. This performance is likely due to the enhanced porosity and surface area resulting from phosphoric acid activation, which favors the adsorption of organic molecules. However, the lower and declining removal efficiency observed for Cu^{2+} suggests that this activated carbon is less suited for metal ion adsorption, possibly due to the lack of specific surface functional groups or structural features required for effective metal binding [62, 90].

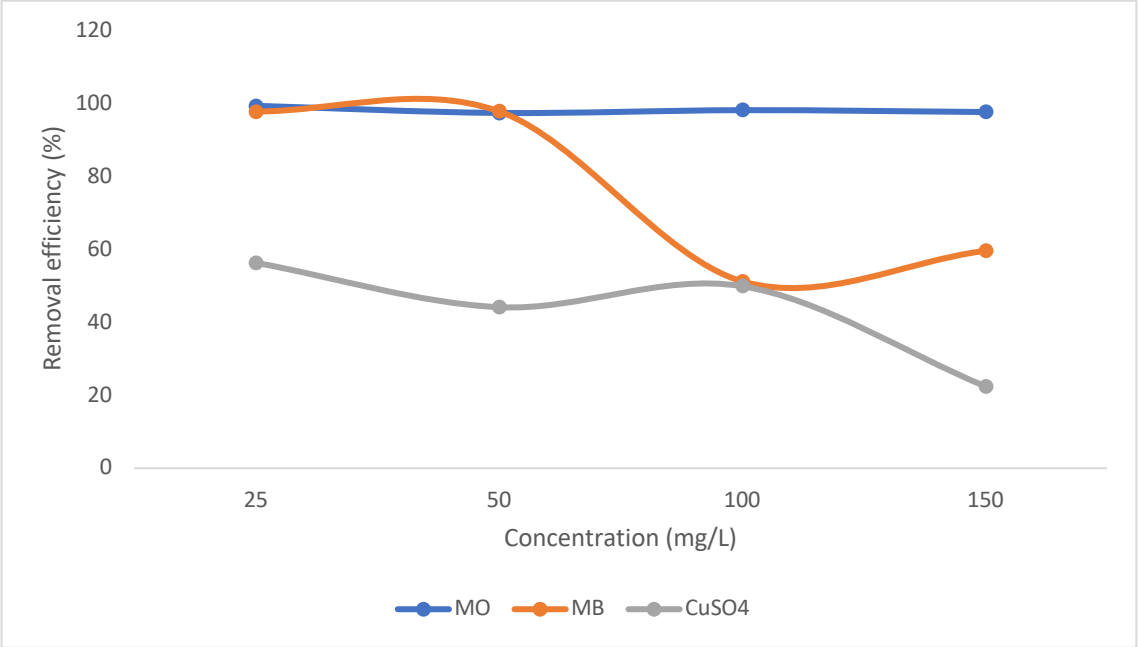

Figure 33: Effect of Concentration on the removal efficiency of MO, MB and Cu^{2+}.

CHAPTER 5: CONCLUSION AND RECOMMENDATIONS

The research demonstrated that activated carbon (AC) derived from waste paper (AC-1 and AC-2) was effective in removing contaminants from domestic wastewater. Analysis showed that AC-2 displayed a higher surface area (678.01 m^2/g) and porosity compared to AC- 1 (455.12 m^2/g), which contributed to its effective adsorption of organic dyes such as methylene blue (MB) and methyl orange (MO). Additionally, the adsorption behaviour of AC-1 aligns best with the Freundlich isotherm, showing an R^2 value of 0.9919, while AC-2 is most accurately described by the Langmuir isotherm, with an R^2 value of 0.9988. Results showed that AC-2 consistently achieved over 90% removal efficiency for turbidity, dissolved oxygen (DO), and organic contaminants at optimal conditions. However, its effectiveness in removing metal ions, specifically copper, was notably lower, with maximum removal efficiencies around 40%. This suggests that while AC-2 is highly effective for organic pollutant adsorption, its structure may require modification to enhance adsorption of metal ions.

The findings further indicated that parameters such as temperature, contact time, and AC dosage had a significant effect on the removal efficiency. For instance, higher temperatures and longer contact times improved the adsorption capacity for MB and MO. Effluent (semi-purified water) treatment displayed lower removal efficiencies compared to influent water, likely due to reduced contaminant concentrations. The commercial AC (AC-3) performed similarly to the prepared ACs, confirming that waste-derived AC could serve as a sustainable alternative for water treatment.

To enhance the application of waste-derived activated carbon (AC) in wastewater treatment, several recommendations are proposed. First, optimising activation conditions, including impregnation ratio and activation time, is essential for

maximising surface area and pore structure, which could improve removal efficiency, particularly for heavy metals like Cu^{2+}. Given the relatively lower adsorption capacity for metal ions, modifications to the AC structure or pore design, including adding metal-binding functional groups, should be considered to increase affinity for heavy metals. Research into the feasibility of scaling up AC production from waste paper is also crucial, as assessing cost, efficiency, and waste management at a larger scale will support practical applications in treatment plants. Additionally, testing the AC on a wider range of contaminants, including other heavy metals and complex organics, would yield a more comprehensive understanding of its adsorption potential. Finally, investigating the use of AC alongside other treatment methods, such as membrane filtration or advanced oxidation processes, could enhance overall contaminant removal efficiency. Together, these efforts underscore the potential of waste-derived AC as an affordable and environmentally friendly solution for diverse wastewater treatment applications, particularly for organic pollutant removal.

References

1. Mustafa R, & Asmatulu E. Preparation of activated carbon using fruit, paper and clothing wastes for wastewater treatment. J Water Process Eng [Internet]. 2020;35:101239. Available from: https://doi.org/10.1016/j.jwpe.2020.101239

2. Saravanan A, Kumar P. S, Jeevanantham S. , Karishma S. , Tajsabreen B. , & Yaashika P. R. Chemosphere Effective water / wastewater treatment methodologies for toxic pollutants removal : Processes and applications towards sustainable development. Chemosphere [Internet]. 2021;280:130595. Available from:

https://doi.org/10.1016/j.chemosphere.2021.130595

3. Khalaf A. Investigation of some physical, chemical, and bacteriological parameters of water quality in some dams in Albaha region, Saudi Arabia. Saudi J Biol Sci. 2021;28:4605–12.

4. Sohrabvandi S, Mousavi P. M, Razavi S. H, & Mortazavian A. M. Application of advanced instrumental techniques for analysis of physical and physicochemical properties of beer: A review. Int J Food Prop. 2010;13:744–59.

5. Singh P. , Sharda S, Cauhan S, Visa M, Nollet H , & Roels M. Domestic waste water treatment by fly and wood ash along with additives materials. Int J Civ Eng Technol [Internet]. 2016;7:67–75. Available from: https://doi.org/10.1016/j.matpr.2019.06.536

6. Bhowmik S , Chakraborty V , & Das P . Batch adsorption of indigo carmine on activated carbon prepared from sawdust: A comparative study and optimization of operating conditions using Response Surface Methodology. Results in Surfaces and

Interfaces [Internet]. 2021;3:100011. Available from: https://doi.org/10.1016/j.rsurfi.2021.100011

7. Stegmann E. Paving the way for recycling. Environmental investment funds of Namibia. 2018, 15-44. https://rnf.com.na/sites/default/files/downloads/EIF-Paving_the_Way_for_Recyling.pdf.

8. Bhatnagar A, Hogland W, Marques M , & Sillanpää M . An overview of the modification methods of activated carbon for its water treatment applications. Chem Eng J [Internet]. 2013;219:499–511. Available from: http://dx.doi.org/10.1016/j.cej.2012.12.038

9. Sousa E , Rocha L , Jaria G & Esteves V . Optimizing microwave-assisted production of waste-based activated carbons for the removal of antibiotics from water. Sci Total Environ [Internet]. 2021;752:141662. Available from: https://doi.org/10.1016/j.scitotenv.2020.141662

10. Benjedim S, Romero-Cano L. A , Pérez-Cadenas A. F, Bautista-Toledo M. I, Lotfi E. M, & Carrasco-Marín F. Removal of emerging pollutants present in water using an E-coli biofilm supported onto activated carbons prepared from argan wastes: Adsorption studies in batch and fixed bed. Sci Total Environ. 2020;720.

11. Han Q, Wang J , Goodman B. A, Xie J, & Liu Z. High adsorption of methylene blue by activated carbon prepared from phosphoric acid treated eucalyptus residue. Powder Technol [Internet]. 2020;366:239–48. Available from: https://doi.org/10.1016/j.powtec.2020.02.013

12. Motaghi H, Arabkhani P, Parvinnia M, & Asfaram A. Simultaneous adsorption of cobalt ions, azo dye, and imidacloprid pesticide on the magnetic chitosan/activated

carbon@UiO-66 bio-nanocomposite: Optimization, mechanisms, regeneration, and application. Sep Purif Technol [Internet]. 2022;284:120258. Available from:

https://doi.org/10.1016/j.seppur.2021.120258

13. Rout P. R, Zhang T.C. , Bhunia P, & Surampalli R.Y. Science of the Total Environment Treatment technologies for emerging contaminants in wastewater treatment plants : A review. Sci Total Environ [Internet]. 2021;753:141990. Available from: https://doi.org/10.1016/j.scitotenv.2020.141990

14. Mushtaq F. , Zahid M. , Bhatti I. A , Nasir S , & Hussain T. Possible applications of coal fly ash in wastewater treatment. J Environ Manage [Internet]. 2019;240:27–46. Available from: https://doi.org/10.1016/j.jenvman.2019.03.054

15. Jjagwe J, Wilberforce P. ,Menya E., & Mpagi H.. Synthesis and Application of Granular Activated Carbon from Biomass Waste Materials for Water Treatment : A Review. J Bioresour Bioprod [Internet]. 2021;6:292–322. Available from:

https://doi.org/10.1016/j.jobab.2021.03.003

16. Nahhal D, El-nahhal I, Najar H , Al-agha M , & El-nahhal Y. Acidity , Electric Conductivity , Dissolved Oxygen Total Dissolved Solid and Salinity Profiles of Marine Water in Gaza : Influence of Wastewater Discharge. 2021;408–28.

17. Shahady T. D. & Cleary W. Influence of a low-head dam on water quality of an urban river system. J Environ Manage. 2021;297.

18. Yan L, Wang Y, Ma H. , Han Z, Zhang Q. & Chen Y . Feasibility of fly ash-based composite coagulant for coal washing wastewater treatment. J Hazard Mater [Internet]. 2012;203–204:221–8. Available from: http://dx.doi.org/10.1016/j.jhazmat.2011.12.004

19. Rashid R, Shafiq I, Akhter P , Iqbal M. J. & Hussain M. A state-of-the-art review on wastewater treatment techniques : the effectiveness of adsorption method. 2021;9050–66.

20. Huang L , Wang L , Wang C , & Tao X. Effect of intercalation of flocculant on adsorption properties of. Inorg Chem Commun [Internet]. 2022;135:109127. Available from: https://doi.org/10.1016/j.inoche.2021.109127

21. Ahmaruzzaman M. Role of Fly Ash in the Removal of Organic Pollutants from Wastewater. 2009;1494–511.

22. Sukmana H, Bellahsen N , Pantoja F. & Hodur C. Adsorption and coagulation in wastewater treatment – Review. 2021;17:49–68.

23. Strauss S. D. Wastewater Management. Power. 1986;130.

24. Aprianti T , Miskah S, Komala R & Hatina S . Heavy metal ions adsorption from pulp and paper industry wastewater using zeolite/activated carbon-ceramic composite adsorbent. AIP Conf Proc. 2018;2014.

25. Sousa E. M, Otero M , Rocha L, Gil M, Ferreira P , & Esteves V. Multivariable optimization of activated carbon production from microwave pyrolysis of brewery wastes - Application in the removal of antibiotics from water. J Hazard Mater. 2022;431.

26.Yadav M, Gupta R, & Sharma R.K. Green and Sustainable Pathways for Wastewater Purification [Internet]. Adv. Water Purif. Tech. Elsevier Inc.; Available from: http://dx.doi.org/10.1016/B978-0-12-814790-0.00014-4

27. Ahmad R, Zaidi S , Aslam A , Arish M, Khan A. Y, & Tariq M. Removal of congo red from water by adsorption onto activated carbon derived from waste black

cardamom peels and machine learning modeling. Alexandria Eng J [Internet]. 2023;71:355–69. Available from: https://doi.org/10.1016/j.aej.2023.03.055

28. Faheem M, Ashraf M , Fazal H , Hafeez A & Hussain M. Journal of Analytical and Applied Pyrolysis Recent trends in activated carbon fibers production from various precursors and applications - A comparative review. J Anal Appl Pyrolysis [Internet]. 2020;145:104715. Available from: https://doi.org/10.1016/j.jaap.2019.104715

29. Delgado N , Capparelli A & Marino D. Pharmaceutical emerging pollutants removal from water using powdered activated carbon : Study of kinetics and adsorption equilibrium. J Environ Manage [Internet]. 2019;236:301–8. Available from: https://doi.org/10.1016/j.jenvman.2019.01.116

30. Corral-Bobadilla M , Lostado-Lorza R, Somovilla-Gómez F & Escribano-García R. Effective use of activated carbon from olive stone waste in the biosorption removal of Fe(III) ions from aqueous solutions. J Clean Prod. 2021;294.

31.Clark R. M. EPA's Drinking Water and Groundwater Remediation Cost Evaluation : Granular Activated Carbon. 2020.

32. Novais R.M, Caetano A.P, Seabra M. P, Labrincha J.A, & Pullar R. C . Extremely fast and efficient methylene blue adsorption using eco-friendly cork and paper waste-based activated carbon adsorbents. J Clean Prod. 2018;197:1137–47.

33.Habeeb O. A, Kanthasamy R, Saber R. E , & Olalere O. A. Characterization of agriculture wastes based activated carbon for removal of hydrogen sulfide from petroleum refinery waste water. Mater Today Proc [Internet]. 2020;20:588–94. Available from: https://doi.org/10.1016/j.matpr.2019.09.194

34. Basheer A. O, Hanafiah M. M, Alsaadi M. A , Al-Douri Y , & Al-Raad A.A. Synthesis and optimization of high surface area mesoporous date palm fiber-based nanostructured powder activated carbon for aluminum removal. Chinese J Chem Eng [Internet]. 2021;32:472–84. Available from: https://doi.org/10.1016/j.cjche.2020.09.071

35. Jjagwe J. , Olupot P. W , Menya E., & Kalibbala H. M. Synthesis and Application of Granular Activated Carbon from Biomass Waste Materials for Water Treatment: A Review. J Bioresour Bioprod [Internet]. 2021;6:292–322. Available from: https://doi.org/10.1016/j.jobab.2021.03.003

36. Lladó J., Gil R. , Lao-Luque C, Solé-Sardans M, Fuente E. & Ruiz B. Highly microporous activated carbons derived from biocollagenic wastes of the leather industry as adsorbents of aromatic organic pollutants in water. J Environ Chem Eng [Internet]. 2017;5:2090–100. Available from: http://dx.doi.org/10.1016/j.jece.2017.04.018

37. Mousavi S.A., Shahbazi D., Mahmoudi A. & Darvishi P . Methylene blue removal using prepared activated carbon from grape wood wastes: adsorption process analysis and modeling. Water Qual Res J. 2022;57:1–19.

38. Nyamful A., Nyogbe E. K. , Mohammed L. , Zainudeen M. N, Darkwa S.A , & Phiri I. Processing and Characterization of Activated Carbon from Coconut Shell and Palm Kernel Shell Waste by H3PO4 Activation. Ghana J Sci. 2021;61:91–104.

39. Hu J, Zhang Q., He C. , Chen Q. L., Qi Z., & Li Q. A multi-stage activated carbon impregnation system: Isotherms, kinetics and multi-objective modeling optimization. Chem Eng Sci [Internet]. 2020;227:115895 https://doi.org/10.1016/j.ces.2020.115895

40. Mohamad Yusop M. F. , Mohd J. E. , & Ahmad M. A. Single-stage microwave assisted coconut shell based activated carbon for removal of Zn(II) ions from aqueous solution – Optimization and batch studies. Arab J Chem [Internet]. 2022;15:104011. Available from: https://doi.org/10.1016/j.arabjc.2022.104011

41. Razmi B. , Ghasemi-Fasaei R. , Ronaghi A , Mostowfizadeh-Ghalamfarsa R. Application of Taguchi optimization for evaluating the capability of hydrochar, biochar, and activated carbon prepared from different wastes in multi-elements bioadsorption. J Clean Prod [Internet]. 2022;347:131292. Available from: https://doi.org/10.1016/j.jclepro.2022.131292

42. Gale M., Nguyen T, Moreno M. , & Gilliard-abdulaziz K. L. Physiochemical Properties of Biochar and Activated Carbon from Biomass Residue : In fl uence of Process Conditions to Adsorbent Properties. 2021;

43. Stone M. T. , & Kozlov M. Separating proteins with activated carbon. Langmuir. 2014;30:80 46–55.

44. Haghbin M. R , & Niknam S. M. Process conditions optimization for the fabrication of highly porous activated carbon from date palm bark wastes for removing pollutants from water. Powder Technol [Internet]. 2021;377:890–9.

Available from: https://doi.org/10.1016/j.powtec.2020.09.051

45. Koyuncu F. ,Güzel F. , & İnal I. G. High surface area and supermicroporous activated carbon from capsicum (Capsicum annuum L.) industrial processing pulp via single-step KOH-catalyzed pyrolysis: Production optimization, characterization and its some water pollutants removal and supercapacit. Diam Relat Mater. 2022;124.

46. Chen P.A. , Cheng H. C. & Wang H. Activated carbon recycled from bitter-tea and palm shell wastes for capacitive desalination of salt water. J Clean Prod [Internet]. 2018;174:927–32. Available from: https://doi.org/10.1016/j.jclepro.2017.11.034

47. Veeraragavan A. , Shanmugavel R. , Abraham N. , Subramanian D. & Pandian S.. Kinetic studies validated by Artificial Neural Network simulation for the removal of dye from simulated waste water by the activated carbon produced from Acalypha indica leaves. Environ Technol Innov [Internet]. 2021;21:101244. Available from: https://doi.org/10.1016/j.eti.2020.101244

48. Raji Y. , Nadi A., Mechnou I. , Saadouni M. , Cherkaoui O. , & Zyade S . High adsorption capacities of crystal violet dye by low-cost activated carbon prepared from Moroccan Moringa oleifera wastes: Characterization, adsorption and mechanism study. Diam Relat Mater [Internet]. 2023;135:109834. Available from: https://doi.org/10.1016/j.diamond.2023.109834

49. Jaria G , Lourenço M. A., Silva C. P. , Ferreira P. , Otero M., & Calisto V . Effect of the surface functionalization of a waste-derived activated carbon on pharmaceuticals' adsorption from water. J Mol Liq [Internet]. 2020;299:112098. Available from: https://doi.org/10.1016/j.molliq.2019.112098

50. Hussain O.A , Hathout, A. S, Abdel-Mobdy Y. E. , Rashed M. M., Rahim E. A. , & Fouzy A. Preparation and characterization of activated carbon from agricultural wastes and their ability to remove chlorpyrifos from water. Toxicol Reports [Internet]. 2023;10:146–54. Available from: https://doi.org/10.1016/j.toxrep.2023.01.011

51. Mareai B. M., Fayed M , Ahmed S , & Ibrahim W. Performance comparison of phenol removal in pharmaceutical wastewater by activated sludge and extended

aeration augmented with activated carbon. Alexandria Eng J [Internet]. 2020;59:5187–96. Available from: https://doi.org/10.1016/j.aej.2020.09.048

52. Tuli F. , Hossain A. , Kibria A. K. , Tareq A. R, Mamun S. M. , & Ullah A. K . Removal of methylene blue from water by low-cost activated carbon prepared from tea waste: A study of adsorption isotherm and kinetics. Environ Nanotechnology, Monit Manag [Internet]. 2020;14:100354. Available from: https://doi.org/10.1016/j.enmm.2020.100354

53. Babas H, Khachani M., Warad I. , Ajebli S. , Guessous A. , & Guenbour A . Adsorption onto activated carbon derived from argan shell residue: Optimization, kinetic, thermodynamic and theoretical approaches. J Mol Liq [Internet]. 2022;356:119019. Available from: https://doi.org/10.1016/j.molliq.2022.119019

54. Gupta V. K. , Gupta B., Rastogi A. , Agarwal S. , & Nayak A . Pesticides removal from waste water by activated carbon prepared from waste rubber tire. Water Res [Internet]. 2011;45:4047–55. Available from: http://dx.doi.org/10.1016/j.watres.2011.05.016

55. Guellati A. , Maachi R., Chaabane T., Darchen A., & Danish M. Aluminum dispersed bamboo activated carbon production for effective removal of Ciprofloxacin hydrochloride antibiotics: Optimization and mechanism study. J Environ Manage. 2022;301.

56. Jaria G., Calisto V., Esteves V. I , & Otero M. Overview of relevant economic and environmental aspects of waste-based activated carbons aimed at adsorptive water treatments. J Clean Prod. 2022;344:1–15.

57. Gratuito M., K., Panyathanmaporn T. , Chumnanklang R., Sirinuntawittaya N. ,& Dutta A . Production of activated carbon from coconut shell: Optimization using response surface methodology. Bioresour Technol. 2008;99:4887–95.

58. Williams N., Oba O. A. & Aydinlik N., P. Modification , Production , and Methods of KOH-Activated Carbon. 2022;164–89.

59. Okada K., Jha V.K., Kameshima Y., Nakajima A. & MacKenzie K., J. Sorption properties of activated carbon derived from used paper and of amorphous $2CaO.Al_2O_3.2SiO_2$ from paper sludge ash. Waste management. 2014. ISBN 1-84564-000-4

60. Ozdemir D., Bulbul S. & Ergun M. Production of activated carbon from waste paper by chemical activation method. International Advanced Researches and Engineering Journal.7(1): 52-61, 2023

61. Rahman A., Hango H. J., Daniel L. S., Uahengo V., Jaime S., J., Bhaskaruni S. V., & Jonnalagadda S., B. Chemical preparation of activated carbon from *Acacia erioloba* seed pods using H_2SO_4 as impregnating agent for water treatment: An environmentally benevolent approach, *Journal of Cleaner Production*, vol. 237, p. 117689, 2019.

62. Daniel L.S., Rahman A., Hamushembe M., N., Kapolo P., Uahengo V., & Jonnalagadda S., B., "The production of activated carbon from *Acacia erioloba* seedpods via phosphoric acid activation method for the removal of methylene blue from water," *Bioresource Technology Reports*, vol. 23, p. 101568, 2023.

63. Kumar P. S., Kirthika K. , Senthamarai V., P., & Mangalaraj S., "Utilization of various agricultural wastes for the production of activated carbon and its application

for the removal of methyl orange from aqueous solution," *Journal of Cleaner Production*, vol. 5, no. 2, pp. 101-108, 2016.

64. Fu F., Wang Q., & Tang L., Impact of industrial discharge on the environment and use of activated carbon for the removal of methyl orange dye from wastewater, *Environmental Chemistry Letters*, vol. 15, no. 3, pp. 475-488, 2017.

65. Almohammadi S. & Mirzaei M., Removal of copper (II) from aqueous solutions by adsorption onto granular activated carbon in the presence of competitor ions, *Advances in Environmental Technology*, vol. 2, pp. 85-94, 2016. doi: 10.22104/aet.2016.392.

66. Langama P., Anguile J., Ndong A., Bouraima A., & Bissielou C., "Adsorption of copper (II) ions in aqueous solution by a natural Mouka smectite and an activated carbon prepared from kola nut shells by chemical activation with zinc chloride ($ZnCl_2$)," *Open Journal of Inorganic Chemistry*, vol. 11, pp. 131-144, 2021. doi: 10.4236/ojic.2021.114009.

67. Krugman H., & Alberts M. (2012) Water demand in the Namibia part of CORB: Cubango-Okavango River Basin Water Audit (CORBWA). Retrieved from http://www.uhydro.de/hywa/_media/en:projects:accounts:cbr7_waterusenam.pdf

68. Obilonu A., Chijioke C., Igwegbe W., Ibearugbulem O., Abubakar Y. (2022). Water Quality Challenges and Impact. Retrieved 22 August 2022, from https://www.scipress.com/ILNS.4.44

69. S. Tiwari. (2015) Water Quality Parameters-A Review. Retrieved 10 June 2022, http://www.ijesird.com

70. WHO. (2011). Guidelines for Drinking-water Quality. Malta: World Health Organization.
https://apps.who.int/iris/bitstream/handle/10665/44584/9789241548151_eng.pdf

71.Ghasemi M., Javadian H., Ghasemi N., Agarwal S., Kumar V. (2016). Microporous nanocrystalline NaA zeolite prepared by microwave-assisted hydrothermal method and determination of kinetic, isotherm, and thermodynamic parameters of the batch sorption of Ni(II). Journal of Molecular Liquids, 215:161-169. DOI: 10.1016/j.molliq.2015.12.038

72. Anirudhan T. S., & Sreekumari S., S. (2011). Adsorptive removal of heavy metal ions from industrial effluents using activated carbon derived from waste coconut buttons. Journal of Environmental Sciences, 23(12), 1989-1998.

73. Borandegi M. & Nezamzadeh-Ejhieh A. (2015). Enhanced removal efficiency of clinoptilolite nano-particles toward Co(II) from aqueous solution by modification with glutamic acid. Colloids Surfaces A Physicochem. Eng. Asp. 479:35–45

74. Palmer C.D., Fish W., & Keely J. F. (1988). Inorganic Contaminants: Recognizing the Problem. In: Proceedings of the 2nd National Outdoor Action Conference on Aquifer Restoration, Ground Water Monitoring and Geophysical Methods, National Water Well Association, Dublin, OH, pp. 555-579.

75. Russell J., Gin J. S., Practical handbook of Soil, vadose zone, and ground - water contamination: *Assessment, Prevention and Remediation*, 2 (1) Washington DC: Lewis publishers, 2004, pp 171 - 180.

76. Jamnicki S., Handke T., Härting M., Lozo B., & Jakovljević M., "Deinking possibilities in the reduction of mineral oil hydrocarbons from recovered paper grades," *Cellulose Chemistry and Technology*, Aug. 2015.

77. Trumić M., & Marković Z., "Separation of ink particles from waste newspaper by deinking flotation," *Journal of Mining and Metallurgy*, vol. 43A, pp. 33-41, 2007.

78. Zhang F., Zhang S., Chen L., Liu Z., & Qin J. (2021). Utilization of bark waste of Acacia mangium: The preparation of activated carbon and adsorption of phenolic wastewater. *Industrial Crops and Products*, *160* , 113157. https://doi.org/10.1016/j.indcrop.2020.113157

79. Bhungthong S., Aussawasathien D., & Hrimchum K. (2018). *Preparation and Properties of Activated Carbon from Palm Shell by Potassium Hydroxide Impregnation : Effects of Processing Parameters*. *45*(1), 462–473.

80. Das M. P., Vijaylakshmi J. V., Suguna P. R., & Karpuramprasad K., "Removal of Methylene Blue by Adsorption Using Fish Scale Chitin," *Nature Environment and Pollution Technology*, vol. 17, no. 3, pp. 993-998, 2018.

81. El-Shafey M., El-Maghraby A., & El-Sayed A. M, "Physical activation of olive stone for production of high surface area activated carbon and its characterization," *International Journal of Environmental Science and Technology*, vol. 17, no. 6,pp.3123-3132,2020.

82. Huang G, Liu Y, Wu X & Cai J, "Activated carbons prepared by the KOH activation of a hydrochar from garlic peel and their CO_2 adsorption performance," *New Carbon Materials*, vol. 34, no. 3, pp. 247–257, 2019.

83. Rouquerol J., *Adsorption by Powders and Porous Solids: Principles, Methodology and Applications*, 2nd ed. Academic Press, 2013.

84. Ankowska H, Swiatkowski A, & Choma J, "Activated Carbon Surfaces in Environmental Remediation, 1991.

85. Torres Lozada P, Amézquita C. P, Agudelo-Martínez M. K, & Ortiz N., Evaluation of turbidity and dissolved organic matter removal through double filtration technology with activated carbon, vol. 85, no. 205, pp. 234–239, 2018.

86. Salam K., Assessment of Surfactant Modified Activated Carbon for Improving Water Quality, Journal *of Encapsulation and Adsorption Sciences*, 9(1), 2019.

87. Utsev JT, Iwar RT, Ifyalem KJ. Adsorption of Methylene Blue from Aqueous Solution onto Delonix regia Pod Activated Carbon: Batch Equilibrium Isotherm, Kinetic and Thermodynamic Studies. J Mater Environ Sci [Internet]. 1058;2020(7):1058–78. Available from: http://www.jmaterenvironsci.com

88. Wongcharee S. Mesoporous activated carbon prepared from macadamia nut shell waste by carbon dioxide activation : Comparative characterisation and study of methylene blue removal from aqueous solution. 2018;(January):1–16.

89. Al-Khaldi, F. A., Abu-Sharkh, B., Abulkibash, A. M., & Atieh, M. A. (2015). Cadmium removal by activated carbon, carbon nanotubes, carbon nanofibers, and carbon fly ash: a comparative study. *Desalination and Water Treatment*, *53*(5), 1417–1429. https://doi.org/10.1080/19443994.2013.847805

90. Nwagbara, V. U., Chigayo, K., Iyama, W. A., & Kwaambwa, H. M. (2022). Removal of lead, cadmium, and copper from water using Moringa oleifera seed biomass. *Journal of Water and Climate Change*, *13*(7), 2747–2760. https://doi.org/10.2166/wcc.2022.091

Appendix

Table 7: percentage yield of prepared Activated carbon (AC)

Activated Carbon	Mass of empty crucible (g)	Mass of crucible + deinked copy paper (g)	Mass of deinked Copy paper (g)	Mass of AC after 0.1% of HCl (g)	% yield
AC-1	45.4	58.7	13.3	1.7	12.8
AC-2	44.1	52.3	8.2	2.0	24.4

Table 8: % Ash of prepared Activated carbon

AC	Mass of empty crucible	Mass of crucible + AC	Mass of AC	Mass of crucible + ash	Mass of AC after furnace	% Ash
AC-1	59.4	60.0	0.6	59.5	0.1	16.67
AC-2	103.6	104.2	0.7	103.7	0.1	14.29
AC-3	67.5	68.2	0.7	67.5	0	0

Table 9: % Volatile of prepared Activated carbon

AC	Mass of empty crucible	Mass of crucible + AC	Mass of AC	Mass of crucible + AC (After furnace)	Mass of AC after furnace	% Volatile matter
AC-1	103.5	104.1	0.6	103.9	0.4	33.33
AC-2	69.7	70.4	0.7	70.3	0.6	14.29
AC-3	103.5	104.5	1.0	104.4	0.9	10

Table 10: Physical characteristics of Activated Carbon

	Activated carbon		
Parameters	**Physical Activation**	**Chemical activation**	**Commercial Activated carbon**
pH	10.94	8.27	7.33
Density g/cm^3	0.94	0.89	1.80
Yield (%)	12.8	24.2	_
Ash Content (%)	16.7	14.29	0
Moisture content (%)	8.5	6.5	0.17

Volatile matter (%)	33.3	14.3	10.0
Fixed Carbon (%)	41.5	64.91	89.83
Acid Solubility (%)	5	0	0
H_20 Solubility (%)	0	5	5

Table 11: Effect of AC-1 dosage on influent wastewater treatment.

Dosage (g)	**Turbidity (NTU)**		**DO (mg/L)**		**TDS (mg/L)**		**Conductivity (µS/cm)**		**Salinity (PSU)**	
		RE (%)		RE (%)		RE (%)		RE (%)		RE (%)
0	355		0.55		785		2384		0.57	
0.05	16.5	95.35	2.92	81.16	692	11.85	1065	55.33	0.50	12.28
0.1	14.8	95.83	3.02	81.79	661	15.80	1017	57.34	0.48	15.80
0.2	16.8	95.26	5.14	89.30	665	15.29	1018	57.30	0.48	15.80

Table 12: Effect of AC-2 dosage on influent wastewater treatment.

Dosage (g)	**Turbidity (NTU)**		**DO (mg/L)**		**TDS (mg/L)**		**Conductivity (µS/cm)**		**Salinity (PSU)**	
		RE (%)		RE (%)		RE (%)		RE (%)		RE (%)
0	355		0.55		785		2384		0.57	
0.05	9.95	97.20	2.64	79.17	681	13.25	1049	56	0.51	10.53
0.1	13.3	96.25	3.06	82.03	680	13.38	1044	56.20	0.49	14.04
0.2	10.9	96.93	3.35	83.58	703	10.45	1083	54.57	0.51	10.53

Table 13: Effect of AC-3 dosage on influent wastewater treatment.

Dosage (g)	**Turbidity (NTU)**		**DO (mg/L)**		**TDS (mg/L)**		**Conductivity (µS/cm)**		**Salinity (PSU)**	
		RE (%)		RE (%)		RE (%)		RE (%)		RE (%)
0	355		0.55		785		2384		0.57	
0.05	18.8	94.70	2.90	81.03	680	13.38	1047	56.08	0.49	14.04
0.1	13.2	96.28	3.19	82.76	690	12.10	1064	55.37	0.50	12.28
0.2	10.8	96.96	4.07	86.48	690	12.10	1064	55.37	0.50	12.28

Table 14: Effect of AC-1 dosage on effluent Wastewater Treatment.

Dosage (g)	**Turbidity (NTU)**		**DO (mg/L)**		**TDS (mg/L)**		**Conductivity (µS/cm)**		**Salinity (PSU)**	
		RE (%)		RE (%)		RE (%)		RE (%)		RE (%)
0	2.31		5.80		698		1594		0.41	
0.05	2.12	8.22	6.21	6.60	509	27.08	785	50.75	0.33	19.51
0.1	1.24	46.32	6.18	6.15	479	31.38	738	53.70	0.31	24.39
0.2	1.55	32.90	6.23	6.90	512	26.65	785	50.75	0.33	19.51

Table 15: Effect of AC-2 dosage on effluent wastewater treatment.

Dosage (g)	**Turbidity (NTU)**		**DO (mg/L)**		**TDS (mg/L)**		**Conductivity (µS/cm)**		**Salinity (PSU)**	
		RE (%)		RE (%)		RE (%)		RE (%)		RE (%)
0	2.31		5.80		698		1594		0.41	
0.05	1.68	27.27	6.05	4.13	531	23.93	814	48.93	0.34	17.07
0.1	1.21	47.62	6.18	6.15	521	25.36	805	49.50	0.34	17.07
0.2	1.75	24.24	6.27	7.50	555	20.49	844	47.05	0.35	14.63

Table 16: Effect of AC-3 dosage on effluent wastewater treatment.

Dosage (g)	**Turbidity (NTU)**		**DO (mg/L)**		**TDS (mg/L)**		**Conductivity (µS/cm)**		**Salinity (PSU)**	
		RE (%)		RE (%)		RE (%)		RE (%)		RE (%)
0	2.31		5.80		698		1594		0.41	
0.05	1.16	49.78	6.23	6.90	524	24.93	806	49.44	0.34	17.07
0.1	1.49	35.50	6.22	6.75	534	23.50	822	48.43	0.34	17.07
0.2	1.94	16.02	6.21	6.60	521	35.36	802	49.67	0.34	17.07

Table 17: Effect of AC-1 contact time on influent wastewater treatment.

Contact time (minutes)	**Turbidity (NTU)**		**DO (mg/L)**		**TDS (mg/L)**		**Conductivity (µS/cm)**		**Salinity (PSU)**	
		RE (%)		RE (%)		RE (%)		RE (%)		RE (%)
0	355		0.55		785		2384		0.57	
10	14.0	96.06	5.95	90.76	605	22.93	930	60.99	0.39	31.59
30	19.8	94.42	5.73	90.40	679	13.50	1044	56.21	0.49	14.04
60	8.32	97.66	3.21	82.87	636	18.98	979	58.93	0.41	28.07
120	11.7	96.70	3.62	84.81	678	13.63	1045	56.16	0.50	12.28

Table 18: Effect of AC-2 contact time on influent wastewater treatment.

Contact time (minutes)	**Turbidity (NTU)**		**DO (mg/L)**		**TDS (mg/L)**		**201508937Conductivity (µS/cm)**		**Salinity (PSU)**	
		RE (%)		RE (%)		RE (%)		RE (%)		RE (%)
0	355		0.55		785		2384		0.57	
10	25.0	92.96	5.76	90.45	708	9.81	1090	54.28	0.51	10.53
30	25.5	92.82	5.76	90.45	687	12.48	1056	55.70	0.50	12.28
60	13.5	96.20	3.04	81.91	675	14.01	1042	56.29	0.44	22.81
120	12.0	96.62	3.75	85.33	696	11.34	1071	55.08	0.51	10.53

Table 19: Effect of AC-3 contact time on influent wastewater treatment.

Contact time (minutes)	**Turbidity (NTU)**		**DO (mg/L)**		**TDS (mg/L)**		**Conductivity (µS/cm)**		**Salinity (PSU)**	
		RE (%)		RE (%)		RE (%)		RE (%)		RE (%)
0	355		0.55		785		2384		0.57	
10	16.7	95.30	5.98	90.80	697	11.21	1074	54.95	0.51	10.52
30	13.4	96.23	4.26	87.09	692	11.85	1064	55.37	0.50	12.28
60	11.4	96.79	3.22	82.92	687	12.48	1057	55.66	0.50	12.28
120	12.1	96.59	3.87	85.79	695	11.46	1069	55.16	0.51	10.52

Table 20: Effect of AC-1 contact time on effluent wastewater treatment.

Contact time (minutes)	**Turbidity (NTU)**		**DO (mg/L)**		**TDS (mg/L)**		**Conductivity (µS/cm)**		**Salinity (PSU)**	
		RE (%)		RE (%)		RE (%)		RE (%)		RE (%)
0	2.31		5.80		698		1594		0.41	
10	1.11	51.95	6.21	6.60	447	35.96	689	56.96	0.29	29.27
30	1.23	46.75	6.23	6.90	505	27.65	779	51.13	0.33	19.51
60	1.14	50.65	6.23	6.90	468	32.95	719	54.89	0.30	26.83
120	1.23	46.75	6.19	6.30	481	31.09	740	53.58	0.31	24.39

Table 21: Effect of AC-2 contact time on effluent wastewater treatment.

Contact time (minutes)	**Turbidity (NTU)**		**DO (mg/L)**		**TDS (mg/L)**		**Conductivity (µS/cm)**		**Salinity (PSU)**	
		RE (%)		RE (%)		RE (%)		RE (%)		RE (%)
0	2.31		5.80		698		1594		0.41	
10	3.73	-61.47	6.27	7.50	525	24.79	808	49.31	0.34	17.07
30	3.85	-66.67	6.18	6.15	527	24.50	812	49.06	0.31	24.39
60	1.60	30.74	6.23	6.90	529	24.21	815	48.87	0.34	17.07
120	1.43	38.10	6.24	7.05	538	22.92	826	48.18	0.35	14.63

Table 22: Effect of AC-3 contact time on effluent wastewater treatment

Contact time (minutes)	**Turbidity (NTU)**		**DO (mg/L)**		**TDS (mg/L)**		**Conductivity (µS/cm)**		**Salinity (PSU)**	
		RE (%)		RE (%)		RE (%)		RE (%)		RE (%)
0	2.31		5.80		698		1594		0.41	
10	0.89	61.47	6.24	7.05	523	25.07	805	49.50	0.34	17.07
30	1.76	23.81	6.25	7.20	518	25.79	793	50.25	0.33	19.51
60	1.07	53.68	6.23	6.90	511	26.79	788	50.56	0.33	19.51
120	1.65	28.57	6.18	6.15	523	25.07	805	49.50	0.34	17.07

Table 23: Effect of AC-1 temperature on influent wastewater treatment.

Temperature (°C)	**Turbidity (NTU)**		**DO (mg/L)**		**TDS (mg/L)**		**Conductivity (µS/cm)**		**Salinity (PSU)**	
		RE (%)		RE (%)		RE (%)		RE (%)		RE (%)
0	355		0.55		785		2384		0.57	
28.0	15.9	95.52	4.77	88.47	707	9.94	1087	54.40	0.51	10.52
40.0	14.0	96.06	6.18	91.10	634	19.24	975	59.10	0.41	28.07
60.0	14.5	95.92	6.00	90.83	613	21.91	943	60.44	0.40	29.82
90.0	13.2	96.28	6.17	91.07	557	29.04	858	64.01	0.36	36.84

Table 24: Effect of AC-2 temperature on influent wastewater treatment.

Temperature (°C)	**Turbidity (NTU)**		**DO (mg/L)**		**TDS (mg/L)**		**Conductivity (µS/cm)**		**Salinity (PSU)**	
		RE (%)		RE (%)		RE (%)		RE (%)		RE (%)
0	355		0.55		785		2384		0.57	
28.0	21.9	93.83	4.16	86.78	703	10.45	1081	54.66	0.51	10.53
40.0	20.9	94.11	6.00	90.83	729	7.13	1122	52.94	0.53	7.02

60.0	22.7	93.61	5.96	90.17	722	8.03	1113	53.31	0.53	7.02
90.0	11.7	96.70	6.07	92	593	24.46	911	61.79	0.38	33.33

Table 25: Effect of AC-3 temperature on influent wastewater treatment.

Temperature (°C)	**Turbidity (NTU)**		**DO (mg/L)**		**TDS (mg/L)**		**Conductivity (µS/cm)**		**Salinity (PSU)**	
		RE (%)		RE (%)		RE (%)		RE (%)		RE (%)
0	355		0.55		785		2384		0.57	
28.0	13.0	96.34	5.93	90.73	694	11.59	1066	55.29	0.50	12.28
40.0	15.7	95.58	6.09	90.97	723	7.90	1112	53.36	0.52	8.77
60.0	16.9	95.24	6.10	90.98	700	10.83	1075	54.91	0.51	10.53
90.0	14.6	95.89	5.90	90.68	609	22.42	936	60.74	0.39	31.58

Table 26: Effect of AC-1 temperature on effluent wastewater treatment.

Temperature (°C)	**Turbidity (NTU)**		**DO (mg/L)**		**TDS (mg/L)**		**Conductivity (µS/cm)**		**Salinity (PSU)**	
		RE (%)		RE (%)		RE (%)		RE (%)		RE (%)
0	2.31		5.80		698		1594		0.41	
28.0	1.50	35.06	6.23	6.90	500	28.37	770	51.69	0.32	21.95
40.0	1.43	38.10	6.17	5.99	481	31.08	742	53.45	0.31	24,39
60.0	1.40	39.39	6.13	5.38	499	28.51	773	51.51	0.32	21.95
90.0	1.56	32.7	6.17	5.99	465	33.38	720	54.83	0.30	26.83

Table 27: Effect of AC-2 temperature on effluent wastewater treatment.

Temperature (°C)	**Turbidity (NTU)**		**DO (mg/L)**		**TDS (mg/L)**		**Conductivity (µS/cm)**		**Salinity (PSU)**	
		RE (%)		RE (%)		RE (%)		RE (%)		RE (%)
0	2.31		5.80		698		1594		0.41	
28.0	1.49	35.50	6.19	6.30	526	24.64	812	49.06	0.34	17.07
40.0	1.44	37.66	6.22	6.75	518	25.79	797	50	0.33	19.51
60.0	1.70	26.41	6.15	5.69	543	22.21	836	47.55	0.35	14.63
90.0	2.08	9.96	6.10	4.92	445	24.64	761	52.26	0.32	21.95

Table 28: Effect of AC-3 temperature on effluent wastewater treatment.

Temperature (°C)	**Turbidity (NTU)**		**DO (mg/L)**		**TDS (mg/L)**		**Conductivity (µS/cm)**		**Salinity (PSU)**	
		RE (%)		RE (%)		RE (%)		RE (%)		RE (%)
0	2.31		5.80		698		1594		0.41	
28.0	1.39	39.83	6.17	5.99	534	23.50	823	48.37	0.35	14.63
40.0	3.41	-47.62	6.16	5.84	523	25.07	807	49.37	0.34	17.07
60.0	1.49	35.50	6.20	6.45	540	22.64	830	47.93	0.35	14.63
90.0	2.63	-13.85	6.18	6.15	507	27.36	781	51.00	0.33	19.51

Instruments used for the characterisation of Activated carbon

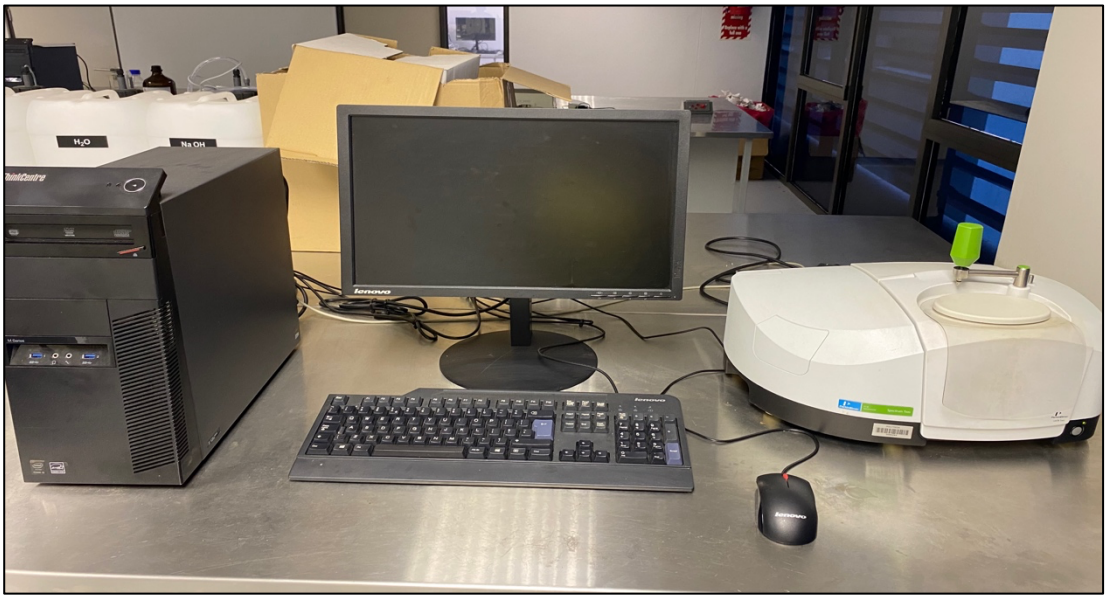

Figure 34: FTIR used for the characterisation of AC

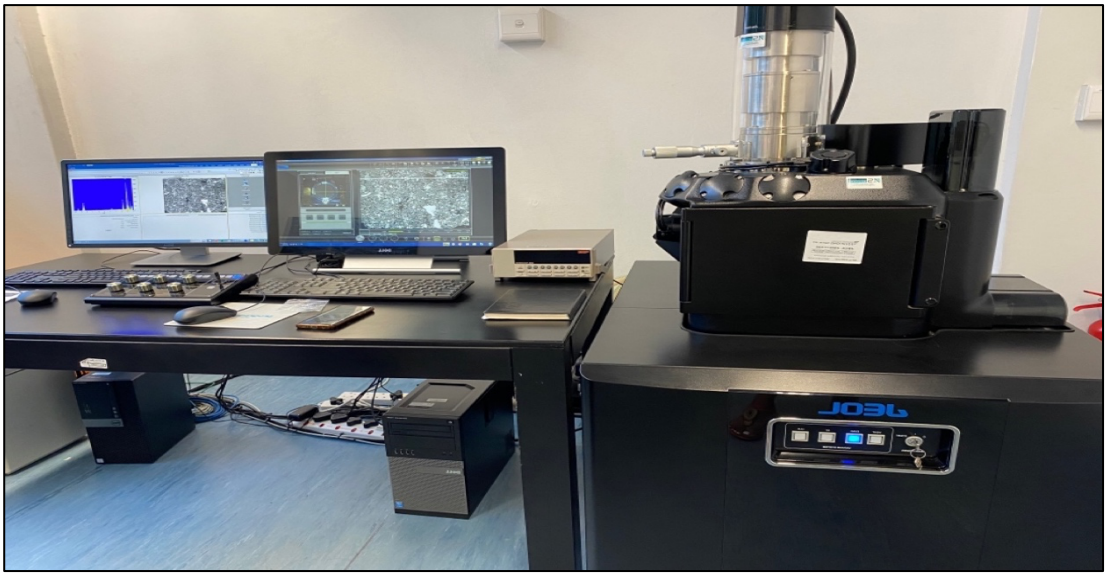

Figure 35: SEM used for the characterisation of AC

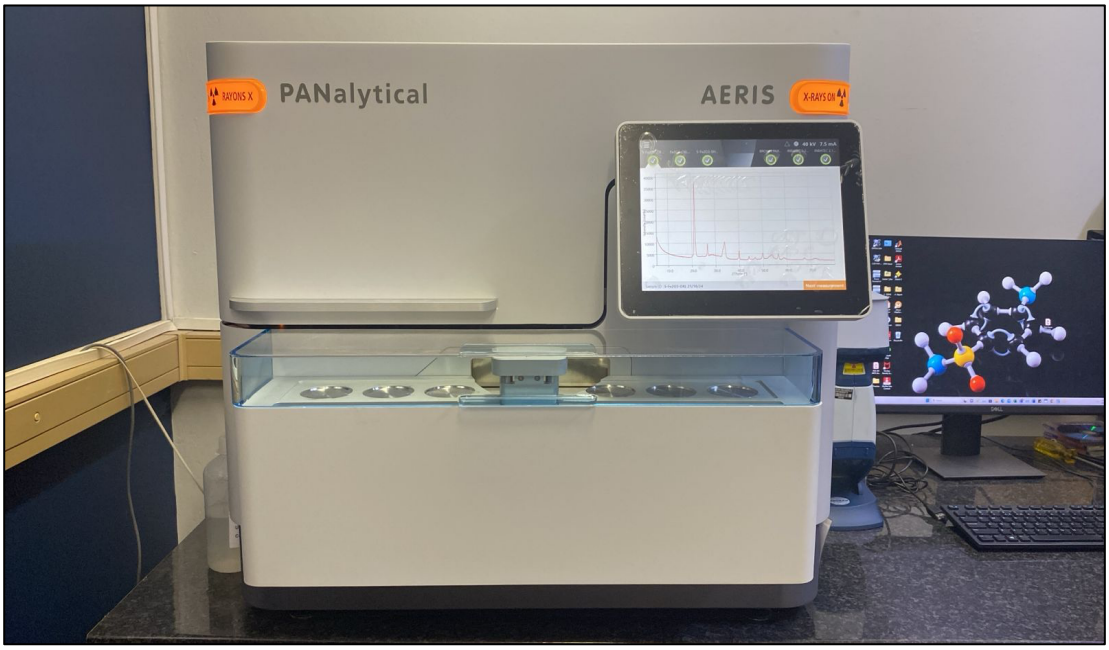

Figure 36: XRD used for the characterisation of activated carbon

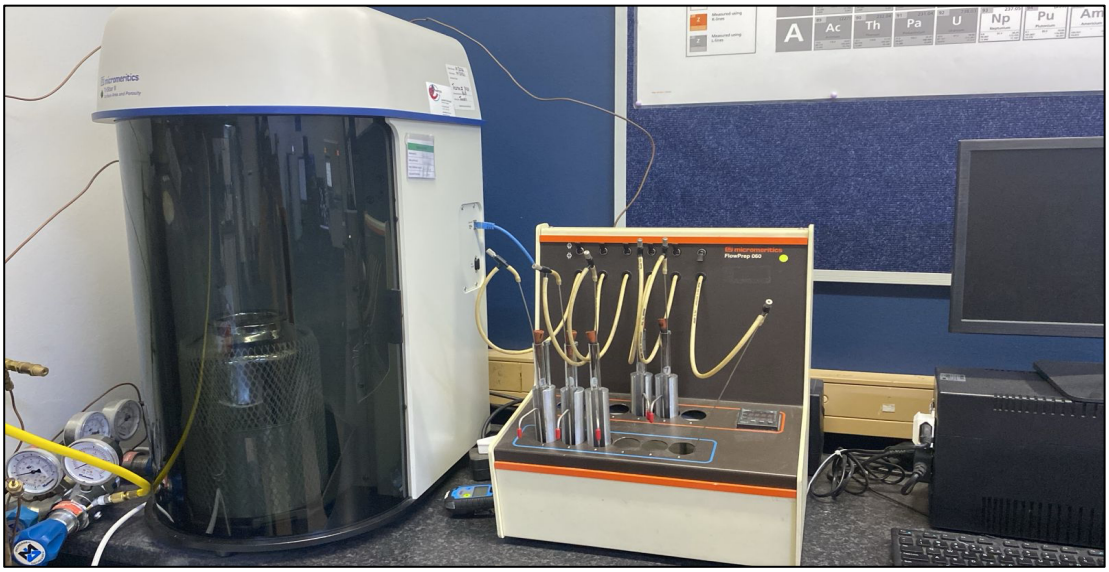

Figure 37: Surface area and porosity using the Brunauer-Emmett-Teller Analysis

Figure 38: UV-Vis Spectroscopy used for absorbances of Cu^{2+}, MO and MB

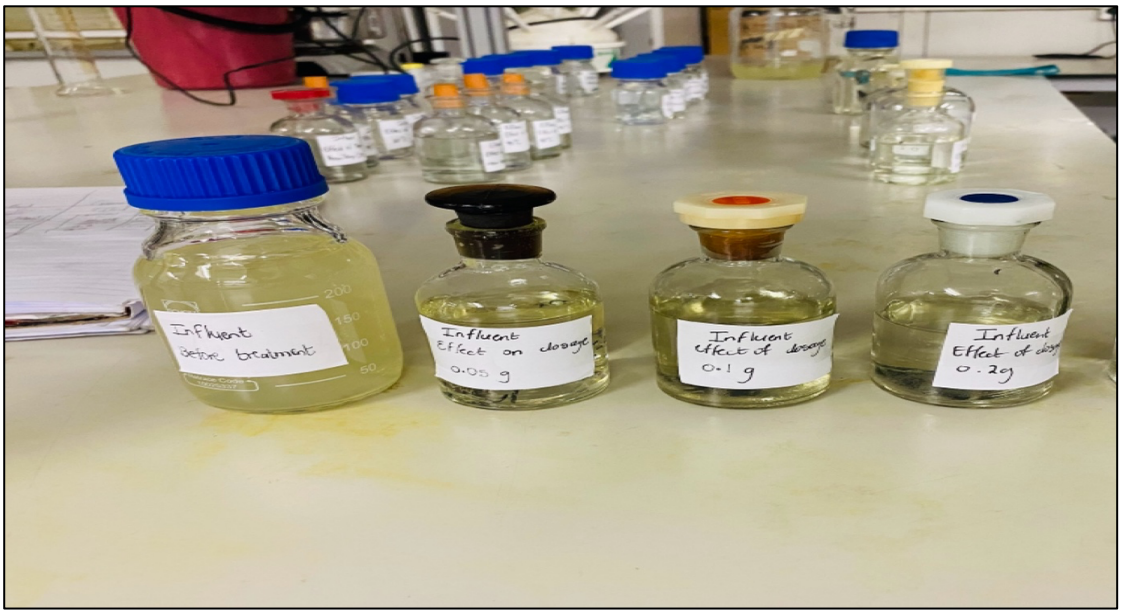

Figure 39: Effect of dosage of AC-2 -Influent before and after treatment with different ACs dosages, ranging from 0.05 - 0.2g.

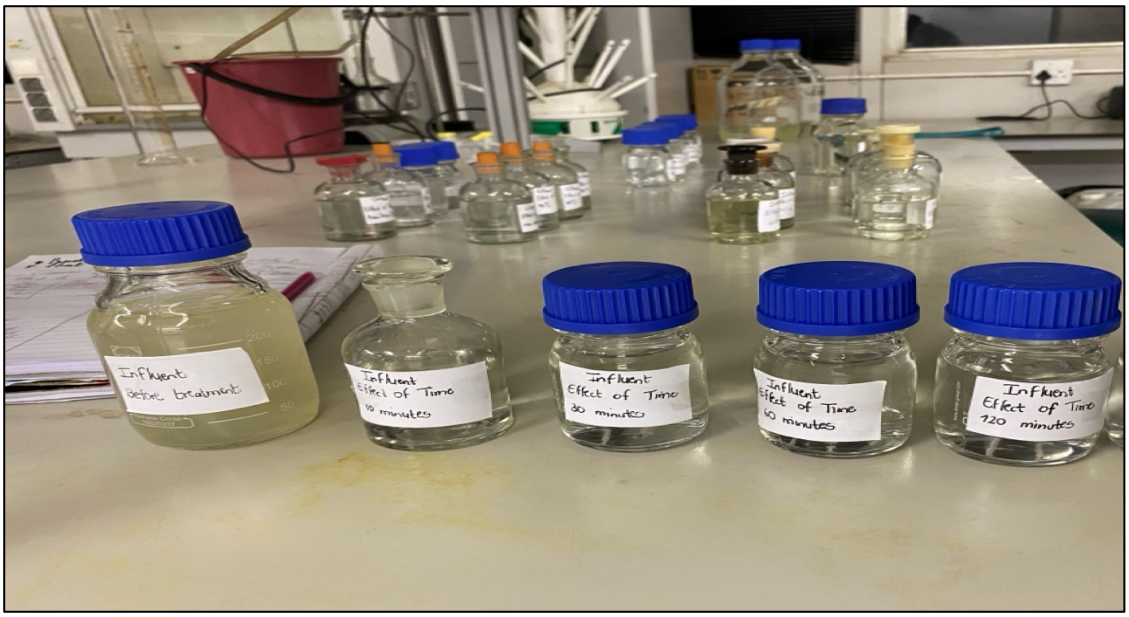

Figure 40: Effect of contact time of AC-2 -Influent before and after treatment with different time intervals ranging from 10 to 120 minutes.

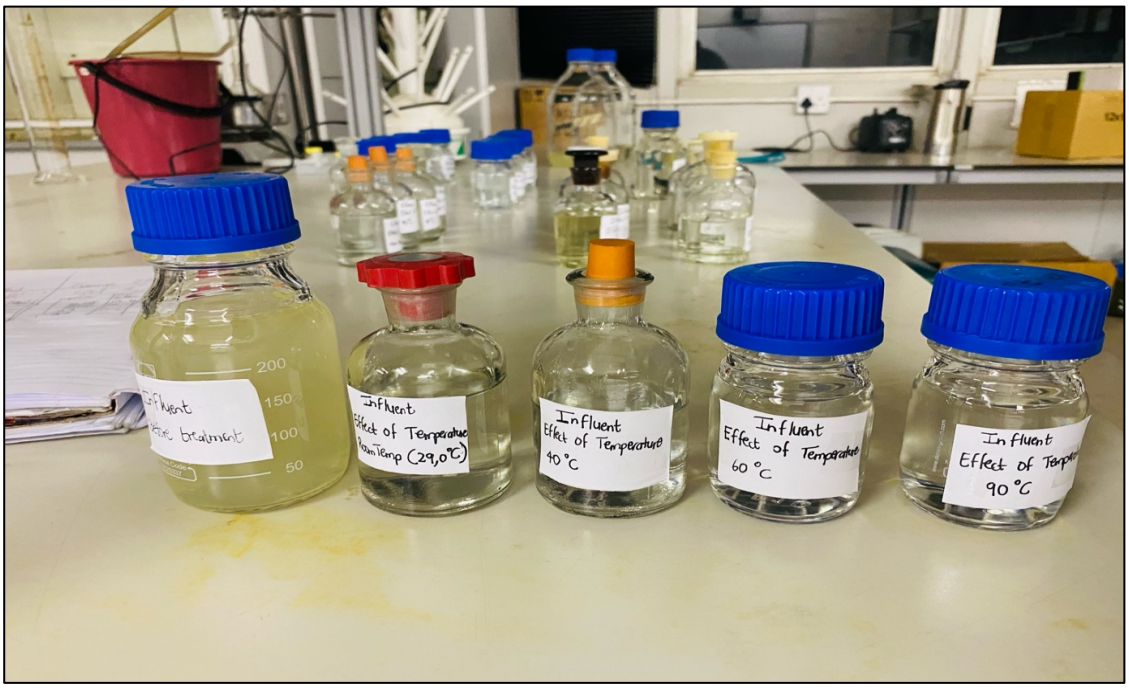

Figure 41: Effect of temperature on AC-2 - Influent before and after treatment across various temperatures, ranging from 28.0 to 90 °C.

Figure 42: Effect of pH on the removal of $CuSO_4$- before and after treatment.

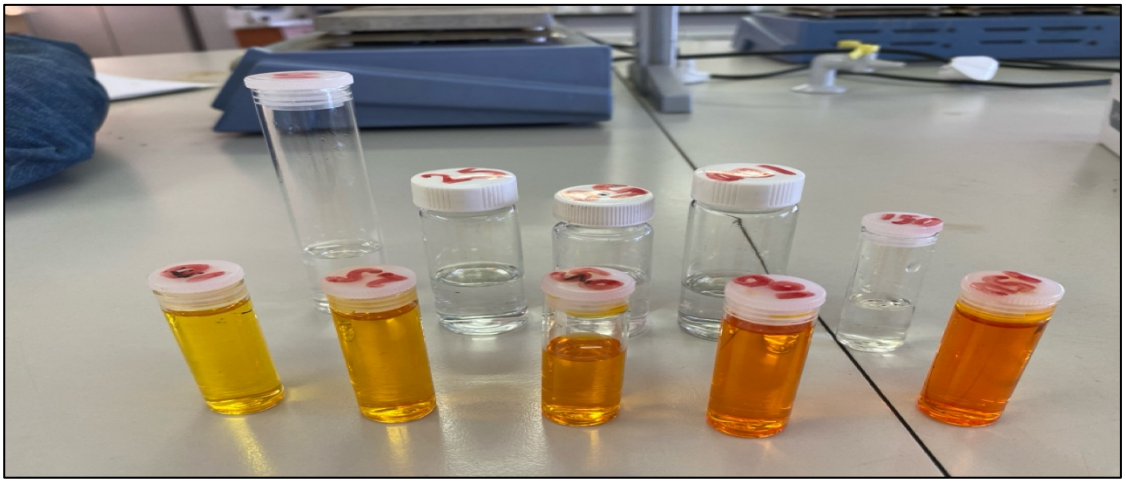

Figure 43: Effect of concentration on the removal of MO- before and after treatment.

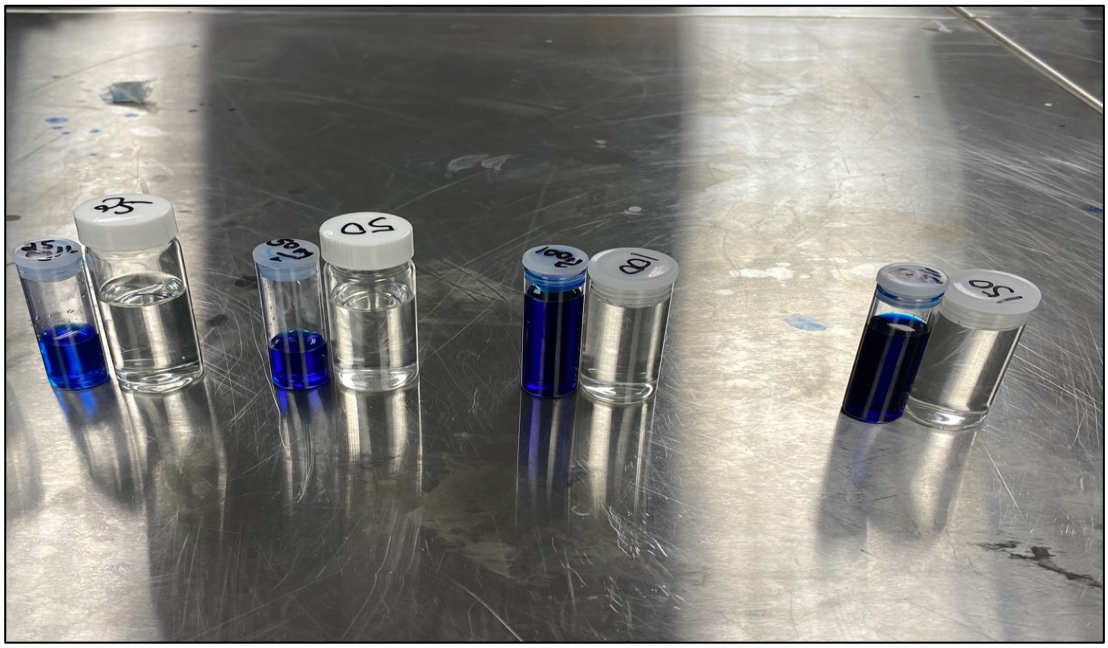

Figure 44: Effect of concentration on the removal of MB- before and after treatment.

CERTIFICATE

OF PARTICIPATION

THIS CERTIFICATE IS PROUDLY PRESENTED TO :

VIOLA-DE-AMOR CHANTALL PATRICIA WILLEMSE

Participated in the 10TH INTERNATIONAL "BAŞKENT" CONGRESS ON PHYSICAL, ENGINEERING, AND APPLIED SCIENCES on October 28-30, 2023 and orally presented the paper entitled

"ACTIVATED CARBON FROM WASTE PAPER FOR THE REMOVAL OF METHYLENE BLUE DYE"

Spc. Leyla ADANMIŞ
Organization Committee Member

Prof. Dr. Revan D. MAN
President of Organization Committee

BZT ACADEMY

Given this on October 28-30, 2023 at Ankara, Turkey.

UNAM
UNIVERSITY OF NAMIBIA

ETHICAL CLEARANCE CERTIFICATE

Ethical Clearance Reference Number: SOS-0101 Date: 18 July 2022

This Ethical Clearance Certificate is issued by the University of Namibia Ethics Committee (REC) in accordance with the University of Namibia's Research Ethics Policy and Guidelines. Ethical approval is given in respect of undertakings contained in the Research Project outlined below. This Certificate is issued on the recommendations of the ethical evaluation done by the ethics committee.

Title of Project: ACTIVATED CARBON FROM WASTE PAPER FOR THE REMOVAL OF CONTAMINANTS FROM WASTEWATER

Student: VIOLA-DE-AMOR CHANTALL PATRICIA WILLEMSE

Student Number: 201408962

Supervisor(s): PROF. ATEEQ RAHMAN
DR. KATHITHILENI KALILI

Centre for Research Services

Take note of the following:

1. Any significant changes in the conditions or undertakings outlined in the approved Proposal must be communicated to the ethics committee. An application to make amendments may be necessary.
2. Any breaches of ethical undertakings or practices that have an impact on ethical conduct of the research must be reported to the ethics committee
3. The Principal Researcher must report issues of ethical compliance to the ethics committee (through the Chairperson) at the end of the Project or as may be requested by the ethics committee
4. The ethics committee retains the right to:

i) Withdraw or amend this Ethical Clearance if any unethical practices (as outlined in the Research Ethics Policy) have been detected or suspected,

ii) Request for an ethical compliance report at any point during the course of the research.

The ethics committee wishes you the best in your research.

Dr. Zivayi Chiguvare (Chairperson Ethics Committee)

Prof. Davis Mumbengegwi (Head, Multidisciplinary Research)

CENTRE FOR RESEARCH SERVICES
Office of the Pro-Vice Chancellor: Research, Innovation & Development
University of Namibia, Private Bag 13301, Windhoek, Namibia
340 Mandume Ndemufayo Avenue, Pioneers Park, Office F223 - Fblock, Second Floor
☎ +264 61 206 4673; E-mail:kmbulu@unam.na; URL.: http//www.unam.edu.na

UNAM
UNIVERSITY OF NAMIBIA

RESEARCH PERMISSION LETTER

Date: 22/11/2022

Student Name: VIOLA-DE-AMOR CHANTALL PATRICIA WILLEMSE

Student Number: 201408962

Programme: Master of Science in Chemistry

Approved Research Title: ACTIVATED CARBON FROM WASTE PAPER FOR THE REMOVAL OF CONTAMINANTS FROM WASTEWATER

TO WHOM IT MAY CONCERN

I hereby confirm that the above-mentioned student is registered at the University of Namibia for the programme indicated. The proposed study met all the requirements as stipulated in the University guidelines and has been approved by the relevant committees.

The proposal adheres to ethical principles as per attached Ethical Clearance Certificate. Permission is hereby granted to carry out the research as described in the approved proposal.

Best Regards

Dr. AEE Shikongo
Head: Postgraduate Support Services
Tel: +264 61 206 3129
E-mail: aeshikongo@unam.na

CENTRE FOR RESEARCH SERVICES
Office of the Director
2022 -11- 22
University of Namibia
UNAM